




Review

Carbon-Based Materials for Supercapacitors: Recent Progress, Challenges and Barriers

Abdul Ghani Olabi ^{1,2,*}, Qaisar Abbas ^{1,3}, Mohammad Ali Abdelkareem ^{1,4,*} , Abdul Hai Alami ¹ ,
Mojtaba Mirzaei ³  and Enas Taha Sayed ⁴

¹ Sustainable Energy & Power Systems Research Centre, RISE, University of Sharjah, Sharjah P.O. Box 27272, United Arab Emirates

² Mechanical Engineering and Design, School of Engineering and Applied Science, Aston University, Aston Triangle, Birmingham B4 7ET, UK

³ School of Computing, Engineering and Physical Sciences, University of the West of Scotland, Paisley PA1 2BE, UK

⁴ Chemical Engineering Department, Faculty of Engineering, Minia University, Minya 61519, Egypt

* Correspondence: aolabi@sharjah.ac.ae (A.G.O.); mabdulkareem@sharjah.ac.ae (M.A.A.)

Abstract: Swift developments in electronic devices and future transportation/energy production directions have forced researchers to develop new and contemporary devices with higher power capacities, extended cycle lives, and superior energy densities. Supercapacitors are promising devices with excellent power densities and exceptionally long cycle lives. However, commercially available supercapacitors, which commonly use high-surface-area carbon-based electrodes and organic solutions as electrolytes, suffer from inferior energy densities due to the limited accessibility of surface area and constrained operating potential window of electrolytes. To address the issue of inferior energy densities, new high-capacity electrode materials and new/state-of-the-art electrolytes, such as ionic liquids, gel polymers, or even solid-state electrolytes, have been developed and evaluated vigorously in recent years. In this brief review, different types of supercapacitors, according to their charge storage mechanisms, have been discussed in detail. Since carbon-based active materials are the key focus of this review, synthesis parameters, such as carbonisation, activation, and functionalisation, which can impact a material's physiochemical characteristics, ultimately affecting the performance of supercapacitors, are also discussed. Finally, the synthesis and applications of different carbon-based materials, i.e., carbon nanotubes, graphene, and activated carbon, have been reviewed, followed by conclusions and outlook.

Keywords: electrochemical energy storage; energy and power densities; carbon-based nanomaterials; nanocomposites; supercapacitors



Citation: Olabi, A.G.; Abbas, Q.; Abdelkareem, M.A.; Alami, A.H.; Mirzaei, M.; Sayed, E.T. Carbon-Based Materials for Supercapacitors: Recent Progress, Challenges and Barriers. *Batteries* **2023**, *9*, 19. <https://doi.org/10.3390/batteries9010019>

Academic Editors: Balaraman Vedhanarayanan and K. C. Seetha Lakshmi

Received: 14 November 2022

Revised: 7 December 2022

Accepted: 15 December 2022

Published: 27 December 2022



Copyright: © 2022 by the authors. Licensee MDPI, Basel, Switzerland. This article is an open access article distributed under the terms and conditions of the Creative Commons Attribution (CC BY) license (<https://creativecommons.org/licenses/by/4.0/>).

1. Introduction

The swift progress in science and technology, coupled with an ever-improving standard of life, has resulted in an increased energy demand. Presently, most of these energy requirements are being satisfied through the deployment of conventional sources of energy [1,2]. These traditional energy resources, such as coal, oil, and gas are depleting drastically, which can result in energy shortages and increased costs in the near future. In addition, these conventional sources are highly polluting and are resulting in higher levels of greenhouse gasses and rising temperatures. To address these environmental concerns arising from these highly contaminating energy sources and to achieve energy security for future generations due to the ever-changing geopolitical scenarios around the globe, a step change is required to reduce the dependence on these traditional energy sources by switching to more renewable and sustainable energy resources like tidal, wind, and solar [3]. These renewable sources can provide an unrestricted supply of energy for generations to come; however, these are intermittent in nature, requiring suitable energy storage

approaches. Many energy storage techniques are used to store excess energy and release this surplus energy when required. Among the different energy storage technologies, electrochemical systems for storing energy, particularly rechargeable batteries and supercapacitors (SCs), have enticed immense concern recently to be utilised as the energy storage system of choice. Lithium-ion batteries are currently the market leaders in the segment of rechargeable batteries, where various battery management systems have been employed to improve their performance and enhance the battery life in real-world applications [4–6]. Moreover, doping has been used as a successful strategy to improve their performance [7]. Rechargeable batteries are considered high energy density devices, whereas SCs are on the opposite end of the spectrum with exceptionally high-power densities. SCs are a preferred choice in many applications due to their exceptional performance characteristics, such as extraordinary high-power densities, extremely rapid charge-discharge rates, good cycle-abilities, and excellent efficiencies [8–10].

SCs have superior power densities; however, these devices retain a moderate level of specific energies. To enhance their energy densities, different strategies have been used, i.e., the use of different electrolytes and electrode materials to enhance their capacitive performance, resulting in improved energy densities. Carbon materials have been modified to enhance their SSA “specific surface area” and optimise the surface chemistry and porous structure. Higher SSA has been achieved through carbonisation and activation under suitable synthesis conditions using different activation agents, whereas surface chemistry is tuned through a heteroatom’s doping such as nitrogen, oxygen, sulphur, and phosphorus. Electrolytes, such as ionic liquids and aqueous solutions, on the other hand, are exploited to achieve higher operating potential windows and superior conductivities, respectively. Moreover, new state-of-the-art electrolytes for commercial devices have been explored to improve operational safety, environmental friendliness, and chemical inertness.

Carbon, transition metal oxides and conducting polymer-based nanomaterials have been widely utilised as electrode active substances for SC’s applications. However, carbon is still the most deployed active material in commercially used supercapacitor devices since using conducting polymers and transition metal oxide-based nanomaterials can result in inferior power densities of SC devices, which is the fundamental advantage for the preferred use of SCs in many high-power delivery applications [11,12]. Carbon-based materials are commonly used in SCs because of their excellent physical, chemical, and electrochemical characteristics including very high surface area, control over porous structures, good electrical conductivities, chemical inertness, structural stability, control of functionalisation, and flexibility of producing a wide range of composites [13,14].

Among different carbon-based materials, AC “activated carbon”, graphene, and CNT “carbon nanotubes” are the most excessively adopted as electrode materials for SCs. Other nanomaterials such as carbon nanofibers, carbon nano-onions, diamond-like carbons, carbide derived carbons, and carbon nano-horns are also being utilised as electrodes in SCs; however, their use is limited to the laboratory testing since these have much higher production costs, restricted scalabilities, and concerns around their environmental affects during production. Even though carbon-based materials have been very successful in a SC’s applications, achieved energy densities are still low ($<10 \text{ Wh kg}^{-1}$). Unlike carbon-based materials, pseudo-capacitive/battery-type materials, such as conducting polymers and transition metal oxides could result in higher energy densities, but power densities and long-term stabilities can be compromised when these materials are used as electrodes in SC cells. To address these concerns, asymmetric or hybrid SCs have recently come under the spotlight for the manufacture of high-performance SCs [15]. The introduction of pseudo-capacitive materials on the surface or within the carbon matrix can result in an improved performance of SCs due to additional Faradic charge storage coupled with fast and fully reversible electronic transfer [16,17]; whereas hybrid devices where anode and cathode are based on pseudo-capacitive/battery-type and carbon-based materials, which can bridge the potential gap to increase the operating window, can also improve a SC device’s efficiency [18,19]. However, these asymmetric or hybrid cell configurations have undesirable

impacts on the power densities and enduring stabilities due to the phase change of active materials and poor reaction kinetics, respectively. Therefore, the fundamental challenge for the scientist is to enhance the energy densities of SCs while preserving their superior power capabilities and cyclabilities. This seems achievable through the enhanced use of carbon with optimised porosity and new, novel electrolyte solutions. Carbon-based substances have been successfully used in SCs over the years and are still very popular in these devices due to a number of advantageous reasons, i.e., improved capacitive performance with control over porous structures, which is based on theoretical and experimental studies [20,21]. Together with conventional characteristics, highly porous carbons with dimensionality ranging from 0D to 3D [22] can be synthesised from a wide range of precursors based on biomasses, polymers, metal organic frameworks, and MXenes [23–26]. These produced carbons can have the following superior structural characteristics: (a) an optimised average pore size (micro-meso pores) for superior charge storage and the efficient movement of electrolyte ions to improve energy densities and retain good power densities, respectively, (b) a large SSA for a large number of adsorption and active sites for electric double layer and pseudo-capacitive charge storage, respectively, (c) an improved surface chemistry through functionalisation to enhance the wettability of the electrode-electrolyte for superior energy storage and good power capabilities, (d) providing a stable and highly conductive platform for long-term stabilities and reduced equivalent series resistance (ESR). Literature on carbon-based materials for a supercapacitor's applications is widely available; however, the fast development in the field of electrochemistry in general, and supercapacitors in particular, requires regular literature updates which can provide summaries of the development of the recent and past, and give an indication of future research direction. Moreover, this review covers some fundamental processes that take place during carbon synthesis, such as carbonisation, activation, functionalisation, and composites preparations, and these processes have not been discussed frequently in literature. Various carbon-based materials used in supercapacitors and their superior characteristics are displayed graphically in Figure 1.

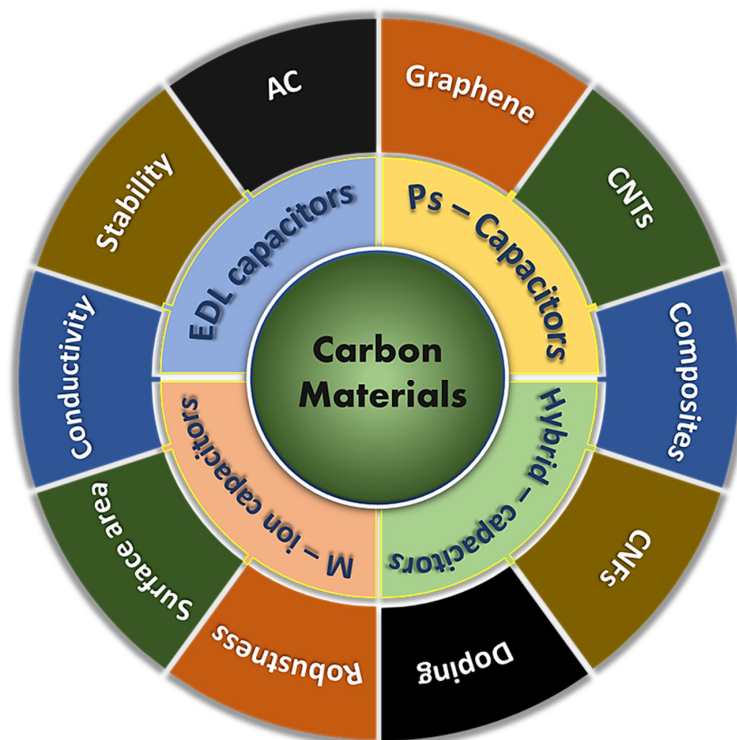


Figure 1. Graphical representation of carbon-based electrode materials and different types of capacitive storage devices.

This brief review will discuss the SC's fundamentals and different configurations. Emphasis will also be directed towards the advancements in synthesising the most commonly used carbon nanomaterials and using various synthesis steps such as carbonisation, activation, functionalisation, and composite production to improve the SC's energy storage capability. Furthermore, the applications of various carbonaceous materials such as AC, graphene, and CNT will be discussed in detail.

2. Different Types of Supercapacitors and Their Energy Storage Mechanism

A supercapacitor is a system that stores energy electrochemically and releases energy by ion adsorption and desorption cycles at the electrolyte-electrode interface. SCs are made up of two electrodes separated by a separator. Supercapacitors are considered to be much superior devices than conventional capacitors because of their higher capacities, enhanced energy densities coupled with a higher power, and faster charge-discharge rates. SCs are classified into two types: symmetric and asymmetric SCs. Asymmetric SC is one in which the two electrodes of the SC are identical, while ASCs "asymmetric supercapacitors" are formed when the two electrodes are made of dissimilar materials, various redox-active electrolytes, or the same substance with various surface functional groups. The symmetric SCs are divided into two groups based on the charge/discharge mechanism of the electrode materials: pseudo-capacitors and EDLCs "electric double-layer capacitors". ASCs are classified in the literature as capacitive ASCs or hybrid ASCs [27]. The former comprises two different capacitive electrodes (similar to those found in EDLCs, while the latter comprises a capacitive electrode and a faradic pseudo-capacitive) electrode. By the beginning of this decade, researchers had introduced all pseudo-capacitive ASCs, which consisted of two different pseudo-capacitive electrodes. Figure 2 depicts these supercapacitor categories.

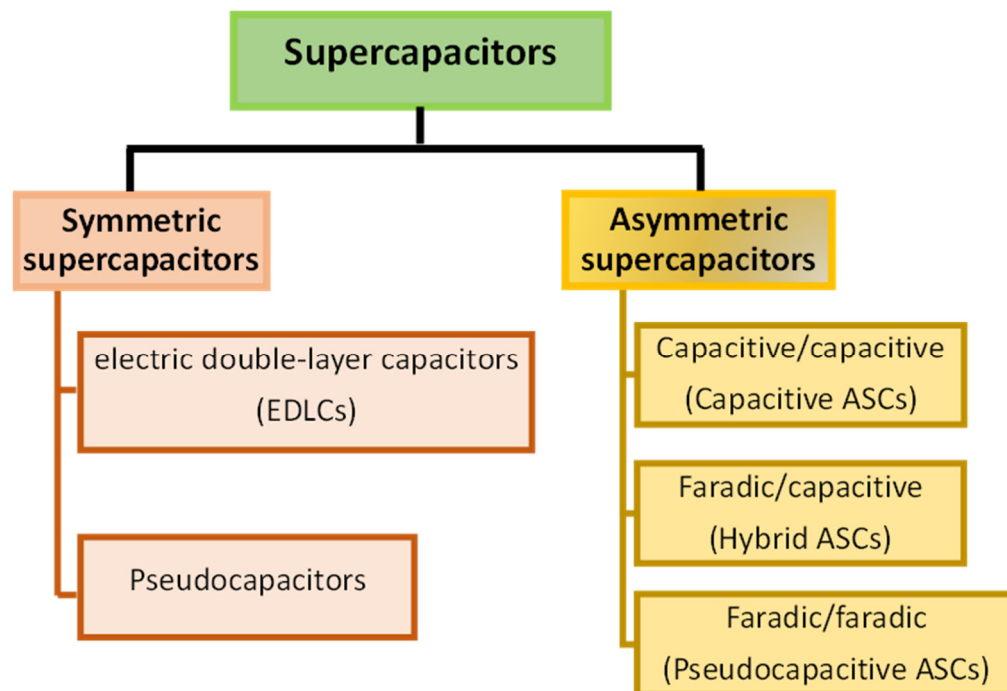


Figure 2. Supercapacitor classifications.

2.1. EDLCs "Electric Double Layer Capacitors"

An EDLC is a type of supercapacitor that physically stores electrical energy at the electrolyte-electrode interface. During the charging-discharging of EDLCs, there is no chemical reaction as the charges are stored physically by the electrostatic attraction; thereby, EDLC has a quick charge-discharge rate, a longer life cycle, and a high-power density [28–30].

The nomenclature of electric double-layer capacitors is associated with the presence of a double layer at the electrolyte-electrode interface when spontaneous charges reorganize when electrically conductive electrodes are immersed in an ionically conductive electrolyte [31,32]. Capacitance is one of the characteristics used to assess a supercapacitor's performance, and it evaluates its ability to store charge. The EDLC's capacitance is related to the available surface area and porous characteristics of the electrode materials [33]. Carbon-based materials with high SSA and good chemical stability, such as graphene, AC, and CNTs, are widely used as electrode materials in EDLCs [34,35]. A commercial carbon-based EDLC has a specific capacitance of approximately 100 to 250 F g⁻¹ and a specific energy density of 3 to 10 Wh kg⁻¹ [31]. Figure 3 depicts a schematic representation of an EDLC.

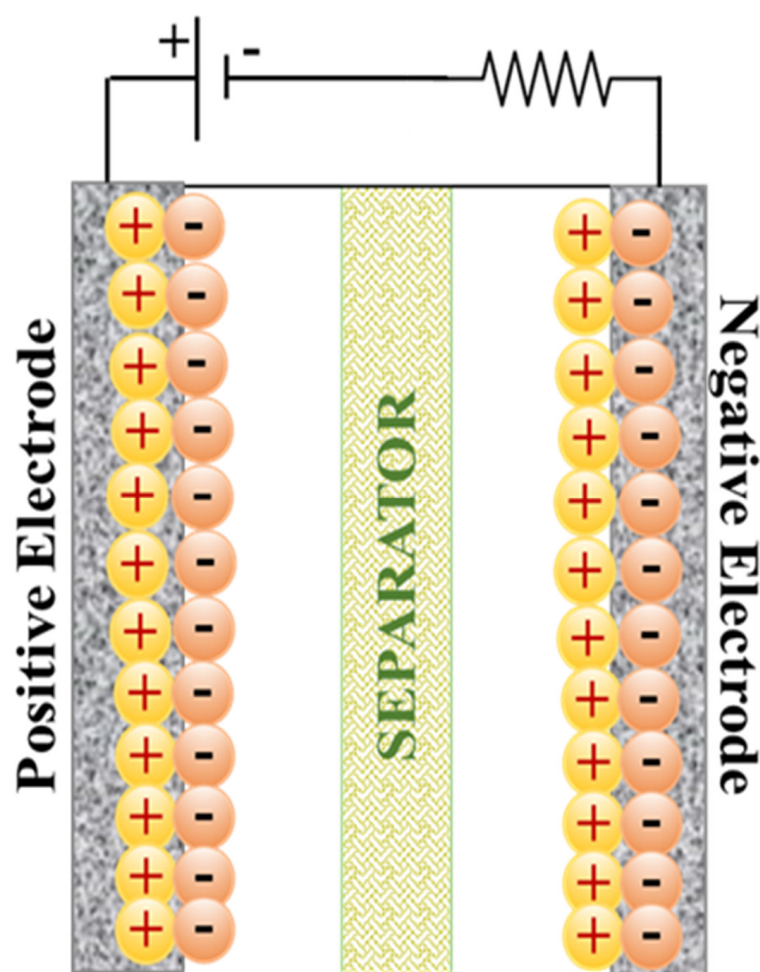


Figure 3. Illustration of EDLC scheme.

2.2. Pseudo-Capacitors (PCs)

PCs, unlike EDLCs, rely mainly on Faradic charge-discharge processes linked with redox reactions. These reduction/oxidation reactions occur at or near the surface of the pseudo-capacitive electrode materials, where electron transfer changes the valence state of the active material [36,37] as seen in Figure 4.

Although both batteries and pseudo-capacitors involve redox reactions, the batteries' cyclic voltammetry (CV) curve has two dominant peaks. The CV curve of pseudo-capacitors has a semi-rectangular shape with two inconspicuous peaks, as shown in Figure 5. As a result, it can be explained on the basis that supercapacitors with pseudo-capacitive electrodes exhibit electrochemical transitional properties between EDLCs and batteries [38].

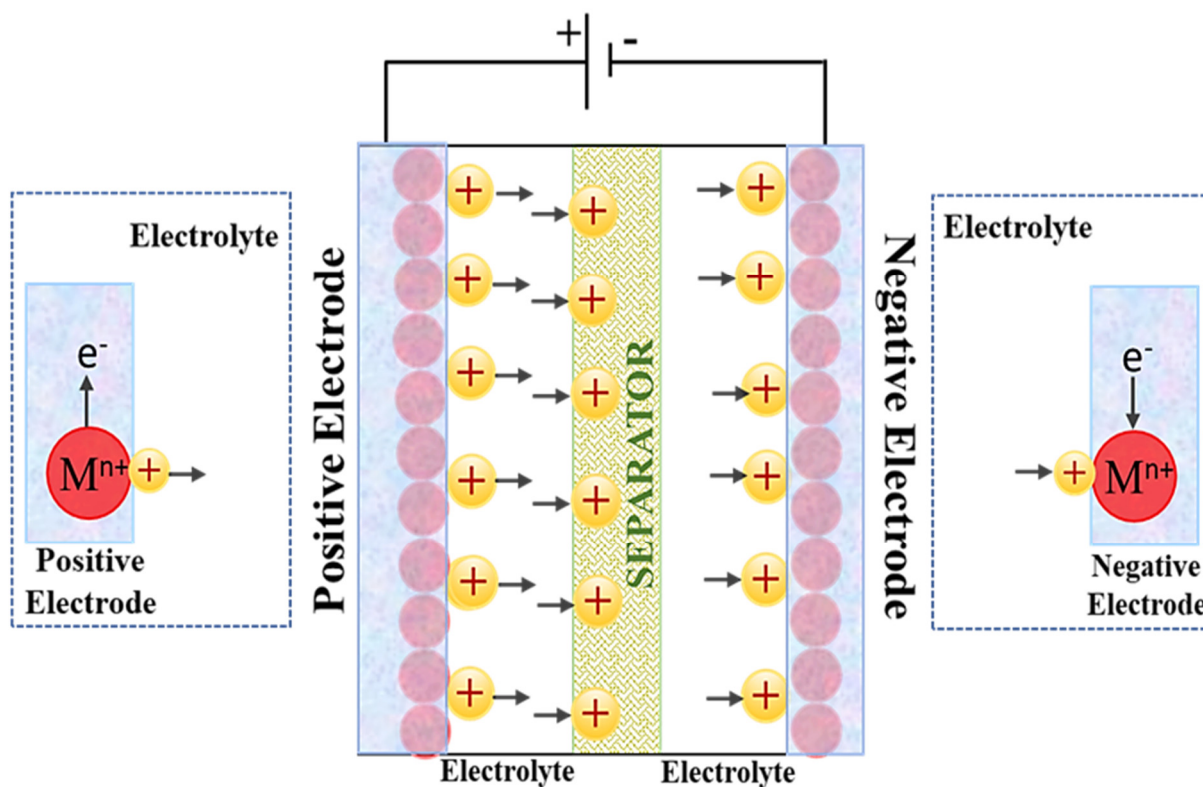


Figure 4. Schematic of the charge storage phenomenon of pseudo-capacitors.

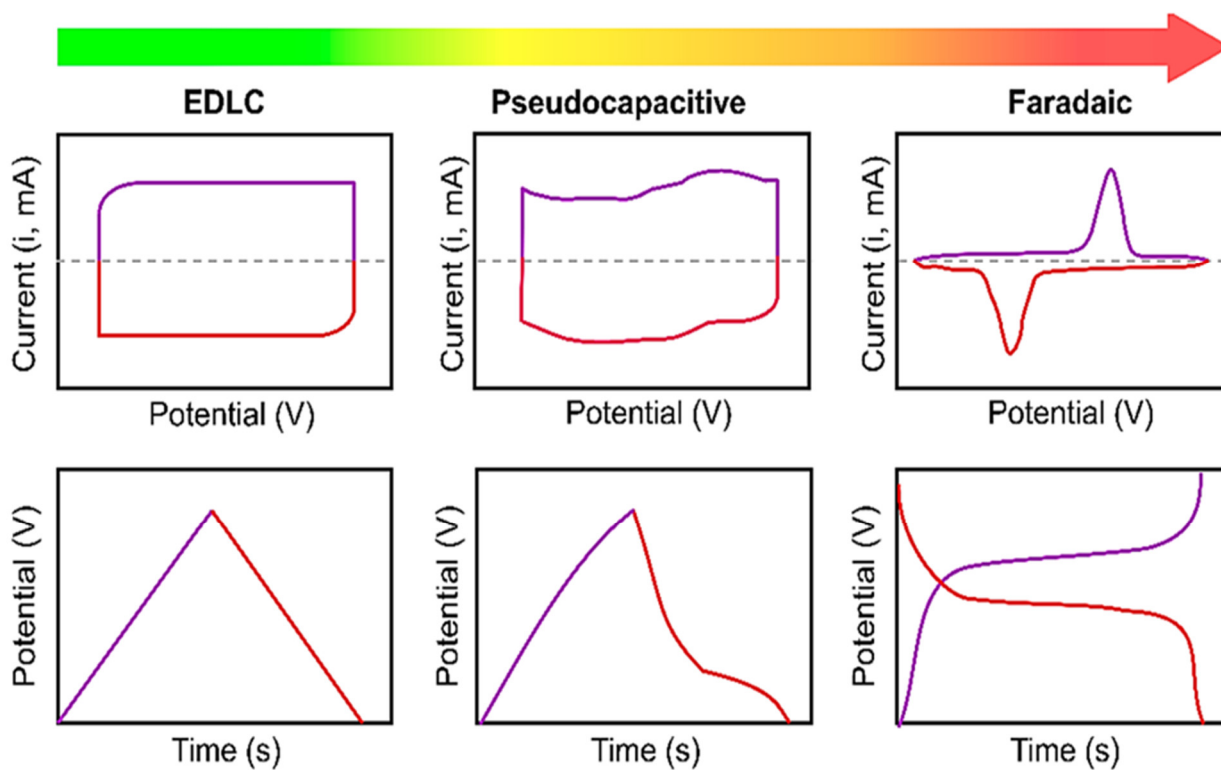


Figure 5. Schematic of typical CVs and corresponding charge-discharge curves of EDLC, pseudocapacitor, and battery-type materials [39], open access.

The charge arrangement at the electrode/electrolyte interface evaluates the charge/discharge process in EDLCs. It excludes redox reactions (no Faradaic process), which explains why the charge-storage process in EDLCs is faster than that in pseudo-

capacitors (the electrochemical double layer is formed in approximately 10^{-8} s in EDLCs, whereas the time constant for redox reactions in pseudo-capacitors is in the range of 10^{-2} to 10^{-4} s) [40]. Different Faradic mechanisms produce three types of pseudo-capacitive electrodes, depicted in Figure 6 with their respective Faradic reactions. In the UPD “underpotential deposition” process, metal ions are electrodeposited at a significantly lower potential than their reversible redox potential onto a substrate, a foreign metal. This process is referred to as electrodeposition. For instance, consider the deposition of H^+ on Pt or Pb^{2+} on Au [41]. Redox pseudo-capacitance occurs at or near the metal-electrolyte interface, where the adsorption of the reduced species H^+ onto the subsurface of oxidized species such as Ru is accompanied by Faradaic charge transfer [42]. The interpolation of ions into the tunnels or layers of the redox-active materials in a Faradic redox system that does not include crystallographic phase change is referred to as pseudo-capacitance. Li^+ , for example, intercalates Nb_2O_5 [43].

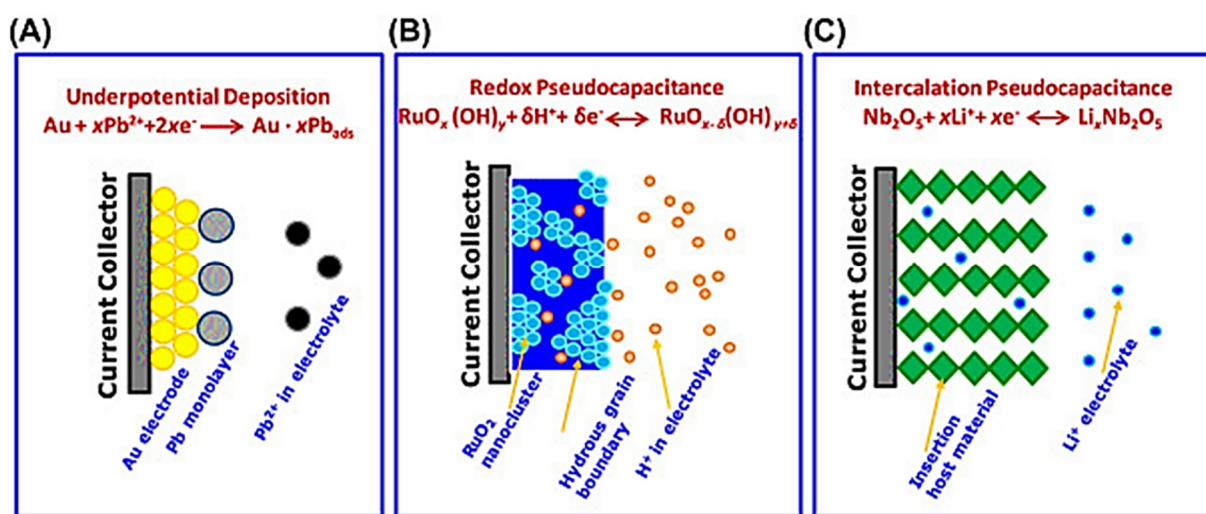


Figure 6. Scheme of the three common types of pseudo-capacitive electrodes, underpotential deposition (A), redox pseudo-capacitance (B), and intercalation pseudo-capacitance, (C) “Reproduced with permission from [44], Elsevier, 2020”.

2.3. Asymmetric supercapacitors

It is possible to compute the specific capacitance of a supercapacitor by using the following equation:

$$C = \frac{S\varepsilon}{D} \quad (1)$$

where ‘ S ’ is the SSA of the active materials, ‘ ε ’ is the relative permittivity, and ‘ D ’ is the EDL thickness. The SSA of the active material in a device is directly proportional to its capacitance, which is why high-surface-area electrodes are used for EDLCs; whereas ‘ D ’ is inversely proportional to the specific capacitance of SCs that give rise to very high capacities of supercapacitors when compared with traditional electrostatic capacitors since the distance ‘ D ’ in SCs is very small compared to that in case of electrostatic capacitors.

It is possible to determine the supercapacitor’s energy density by using Equation (2), which is as follows:

$$E = \frac{1}{2}CV^2 \quad (2)$$

C represents the capacitance window, and V accordingly represents the operating voltage window. Equation (3) gives the power density, or the amount of energy released in a given amount of time:

$$P = \frac{1}{4} \frac{(\Delta V)^2}{R} \quad (3)$$

where “ V ” stands for the potential operating window, and “ R ” is the equivalent series resistance (ESR), which comprises the resistance of the dielectric material, the current collector, the electrolyte, and the electrode. This is one of the fundamental reasons that EDLCs deliver higher power densities compared with pseudo-capacitors, since carbon has lower resistances when compared with pseudo-capacitive materials.

According to Equation (2), if a two-fold increase in the voltage window can be produced, a four-fold excess in energy density can be obtained. A well-designed asymmetric supercapacitor can provide a wider voltage window. The two distinct potential windows of the two electrodes could be combined to produce the full device’s wide voltage window. The CV curves of capacitive and hybrid asymmetric supercapacitors are shown in Figure 7 [45]. The structure and materials used to make the electrodes are critical in attaining high energy and power densities in capacitive and hybrid asymmetric SCs.

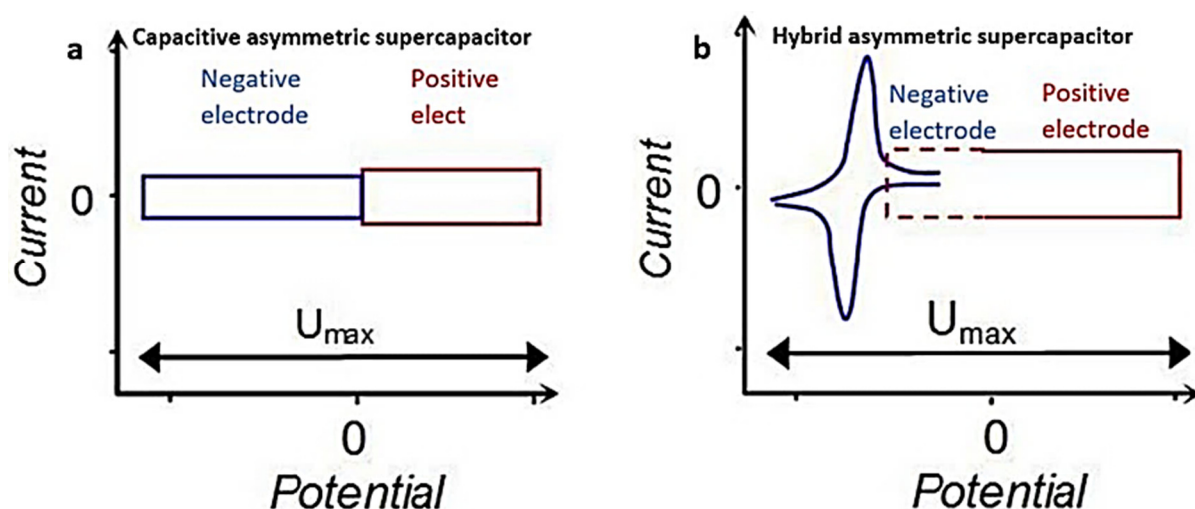


Figure 7. Schematic illustration of the CV curves for (a) capacitive asymmetric SC and (b) hybrid asymmetric SC [45], open access.

2.4. MICs “Metal-Ion Capacitors”

In recent years, improved hybrid electrochemical energy storage (EES) devices known as metal ion capacitors (MICs), have been developed to address the power density and cycle life issues of LIBs as well as the low energy density of SCs. These MICs share many characteristics with LIBs and SCs (Figure 8), and are made up of a battery-type anode (electrochemical intercalation or conversion) and a capacitor-type cathode (physical adsorption) in an electrolyte containing metal ion. The electrode materials used in MICs significantly impact their electrochemical performance, and a wide variety of materials have been tried [46–48]. Ion capacitors are classified into several types based on the metal ion electrolytes used, including LICs “lithium-ion capacitors”, SICs “sodium ion capacitors”, PICs “potassium ion capacitors”, ZICs “zinc ion capacitors”, MnICs “magnesium ion capacitors”, CICs “calcium ion capacitors”, and ALCs “aluminium ion capacitors” [46]. The cathode and anode, respectively, use physical (adsorption/desorption) and chemical (intercalation/deintercalation or conversion) processes to store and release energy when charging and discharging the MICs [47,48]. MICs have several advantages over conventional SCs due to the combination of two energy storage systems in one device, including (1) an increased energy density and battery capacity, (2) a higher power density compared to LIBs, (3) a large working temperature range of -25 to 80 °C, and (4) less self-discharge characteristics compared to SCs [49,50]. Different MICs have so far successfully shown a trade-off between SCs and batteries [51,52]. The present MICs are far from adequate because of the imbalance in the electrode kinetics and capacities of the two electrodes [53,54]. In most circumstances, lower charge and discharge rates result in a higher energy density,

whereas high charge and discharge rates, or a lengthy cycle life, result in a much lower energy density.

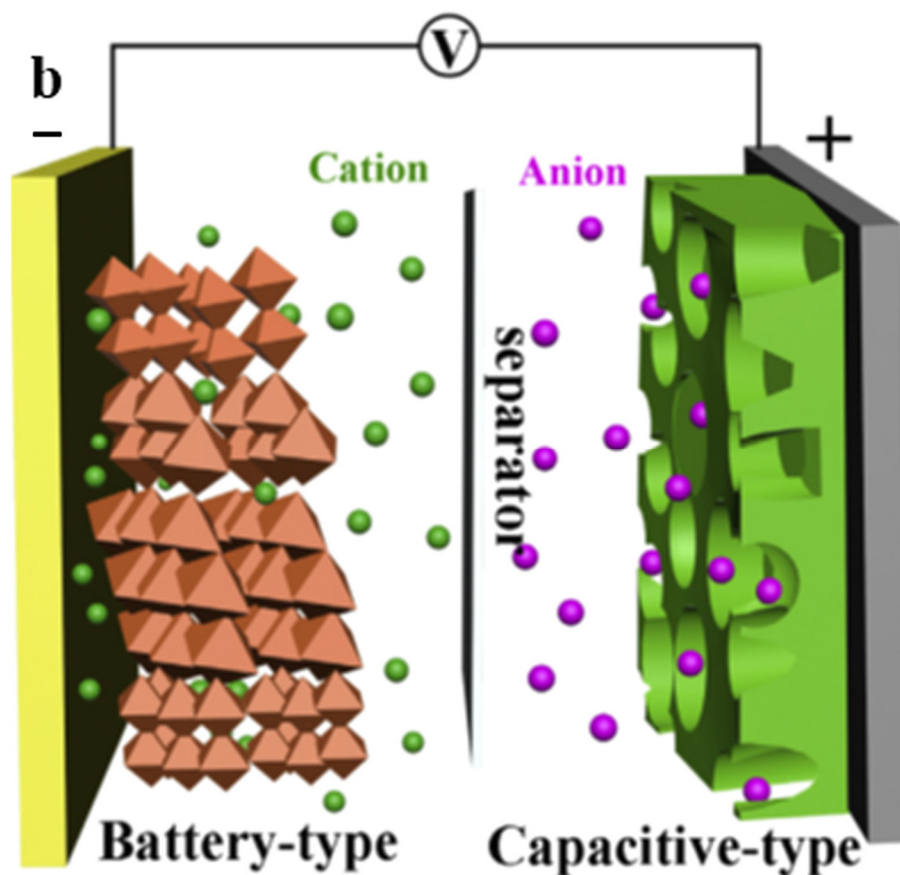


Figure 8. Scheme of the metal ion supercapacitor, “Reproduced with permission from [54], Elsevier, 2021”.

A wide variety of electrode and electrolyte materials are used for SC applications. Particularly, there is a very wide range of active materials ranging from carbons to conducting polymers and transition metal oxides that have been utilised in SCs. However, commercially available SCs still predominantly use carbon-based materials—activated carbon, to be precise. The following section will discuss the synthesis, characterisation, and application of different and some of the most commonly used carbon-based materials.

3. Carbon-Based Electrode Active Materials Synthesis Process

A wide range of carbon-based nanomaterials have been synthesised and adopted as active materials in energy conversion and storage devices, particularly as electrode materials in SCs. Among these materials, AC [55], Gr “Graphene” [56], CNT [57] and CNF “carbon nanofibers” [58] are some of the leading nanomaterials used for supercapacitor applications. Carbon-based nanomaterials are extensively used because of their extraordinary attributes, such as their large SSA, high electrical conductivity, control over porous structure, cost-effectiveness, large-scale production, and ease of their modification both in terms of chemical and physical characteristics. There are several procedures, such as carbonisation, activation, functionalisation, and doping, that are being used to fine tune their physical and chemical characteristics, which can significantly influence the electrochemical performance of SCs when these carbon-based nanomaterials are employed as electrodes. These processes will be covered in detail in the following sub-sections.

3.1. Carbonisation

Carbon-based materials are produced through the high-temperature pyrolysis of either biomass-based or synthetic precursors under inert conditions using a constant flow of inert gasses such as argon or nitrogen. The optimum carbonisation temperature range of 700–1000 °C is commonly utilised to produce carbon materials, whereas temperatures beyond 1000 °C are rarely used due to high material burnout and collapse of a porous structure, resulting in low yield and low level of porosity, respectively, at elevated temperatures [59]. Fundamentally, carbonisation is a thermal decomposition process that transforms precursors into carbon or carbon-containing residues when treated at very high temperatures in an inert environment. The final carbon product and its quality can be impacted by various carbonisation parameters such as pyrolysis temperature, carbonisation time, ramping rate, and condition/type of precursors. Based on synthesis temperature, carbon can be categorized as non-graphitic or graphitic, where non-graphitic carbons are usually the preferred choice as electrodes in supercapacitor applications due to their high level of porosity and three-dimensional crosslinked structure. Whereas graphitic carbon is preferred for its utilisation in batteries, especially lithium-ion batteries, due to its superior intercalation properties. Studies have shown that increasing the pyrolysis temperature can result in an increased level of porosity and wider pore sizes; however, carbonisation temperatures beyond 800 °C can decrease porosity and average pore sizes due to the collapse of the porous structure of the precursor. Nevertheless, when these carbon precursors are treated at exceptionally high temperatures, i.e., above 2500 °C, they can go through the fluid phase, which can produce graphitic carbon with a well-aligned and crystalline graphitic structure, reducing porosity dramatically. Carbons treated at lower temperatures have three-dimensionally crosslinked structures unlike graphitic carbon, which gives rise to high levels of porosity and can be highly useful for a wide range of applications, i.e., electrochemical energy storage applications, especially as active electrode materials in SCs.

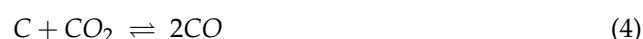
3.2. Activation

Carbons produced through the pyrolysis of various precursors result in generating nanomaterials with a wide range of porous structures, i.e., pore sizes, pore volumes, and specific surface areas. Applicability of all these porous materials with diverse characteristics depends on the accessibility of the pores of the produced carbon [59]. Open pores can be useful for enhancing the accessibility of the surface area to external fluids, such as electrolyte solutions in the case of the supercapacitor. On the other hand, closed pores can only influence the physical features, such as mechanical strength, bulk density, and thermal conductivity, of carbons. An open pore that can be accessible to external fluids can have numerous shapes and sizes. In terms of the sizes of pores, these can be classified into micro, meso, or macropores. Whereas these pores can exist in a wide range of shapes, such as bottle neck pores, blind pores, micro pores with one end closed, slit type pores, and interconnected pores with both ends open.

The level of porosity of these carbon materials can be enhanced even further by using a process known as activation. By using this technique, closed pores can be opened, existing open pores can be widened, and further new porosity can be created through partial oxidation using oxidation agents. Activation can be categorised into two types of chemical and physical activation depending on activation agents, temperature range, and the involved chemical processes. Physical activation is slightly more desirable as it is safer and provides activated carbon with better control over porosity. Physical activation is a process with two-steps: the first step is carbonisation under inert conditions, followed by activation through the introduction of an activation agent [60]. In the case of physical activation, air, steam, carbon dioxide, or a mixture of these is utilised as the activation agent. However, carbon dioxide is the most popular activation agent since the activation process can be controlled better by controlling the flow rate, activation time, and temperature. Physical activation is normally performed in the temperature range of 700–1200 °C. Even

though higher activation temperatures and extended periods of activation times can result in a very high level of porosity, these can also result in a very high degree of burn-off [61].

During the activation process, the active oxygen removes more reactive portions from the carbon skeleton in the form of CO and CO₂, resulting in the formation of new pores and the widening of the pores created through carbonisation. The level of porosity, porous structure (pore size, SSA, and pore volume), and the degree of burn-off in the resulting activated carbon depend upon the activation temperature, heating rate, and activation time. Additionally, the rate of burning out of the carbon skeleton varies depending on where on the exposed surface it occurs [62]. The activation reactions when carbon is activated using carbon dioxide or steam as activation agents can be represented by Equations (4) and (5).



Additional rationales for the preferred choice of physical activation include narrow pore size distribution of the resultant carbon and control over-involved reactions. Furthermore, it provides better control over the level of functional groups on the carbon surface.

Chemical activation is different in that it involves only one step for carbonisation and activation, unlike physical activation. Activation agents, such as phosphoric acid, potassium hydroxide, and zinc chloride are used to saturate precursors followed by chemical activation; however, the temperature range is much lower, being in the range of 400–600 °C. Washing is added as an extra step that is applied to remove any excess chemical agent left during the activation [63].

Even though there are several drawbacks to chemical activation, it still carries numerous benefits. It is less energy intensive since it is a one-step process and does not involve carbonisation; moreover, it requires much lower activation temperatures. It has also been observed in numerous studies that chemical activation can result in a higher level of porosity. In a study by Zhang, Lixing, et al., they activated agar through a one-step chemical activation process, employing an activation agent, KOH. The activation created a large number of three dimensional interconnected voids resulting in high levels of porosity as seen in Figure 9a,b. As a result, higher levels of pore volume and an SSA of 0.81 cm³ g^{−1} and 1672 m² g^{−1}, respectively, were achieved which were much higher than the 0.47 cm³ g^{−1} and 1048 m² g^{−1} achieved using the traditional two-step physical activation, respectively, as seen in Figure 9c,d [64].

3.3. Functionalisation

By inserting functional groups on the surface or within the structure of carbon-based active materials, the capacitive characteristics of EDLCs can be improved. This improvement in capacitive performance is due to additional pseudo-capacitive contributions made by functional groups such as sulphur (S), nitrogen (N), phosphorus (P), boron (B), and oxygen (O). Functional groups can be introduced on the carbon surface through post-treatment with heteroatom-containing materials or through self-doping by carbonising the heteroatom-rich precursors [65]. For instance, treatment of prepared carbon with ammonia can result in surface nitrogen-rich carbons, whereas carbonisation of materials such as urea or melamine can result in introducing nitrogen on the surface and within the carbon metrics [66]. Nitrogen functionalised carbons are the most investigated since these not only enhance the capacitive performance of SCs but also enhance the surface wettability, especially towards aqueous solutions. Furthermore, nitrogen functionalised carbon can be used either as aqueous or organic electrolytes, unlike oxygen heteroatoms doped carbon, which cannot be used with aqueous electrolytes [67]. Figure 10 is the graphical representation of carbon materials doped with different functional materials, i.e., B, N, S, and P.

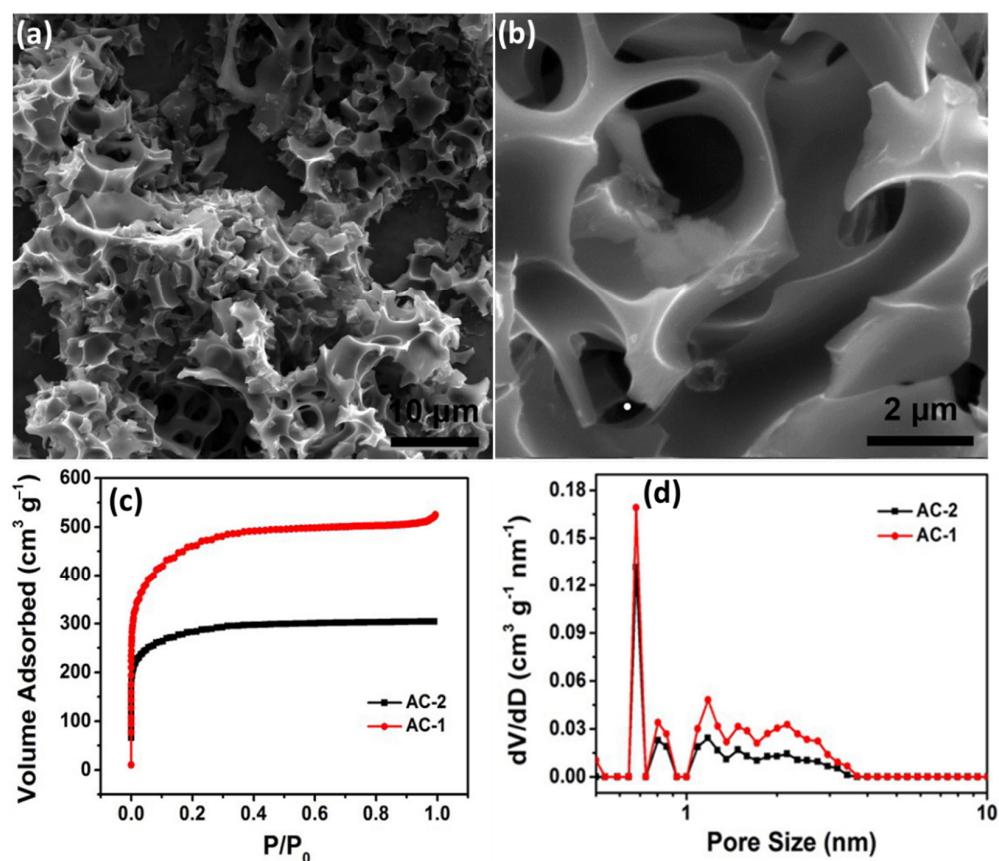


Figure 9. (a) The SEM micrograph at low resolution and (b) high resolution. (c) The nitrogen adsorption-desorption isotherms of AC-1 (chemically activated) and AC-2 (physically activated) and (d) the pore size distribution of AC-1 and AC-2. Reproduced with permission from [64], Elsevier, 2018.

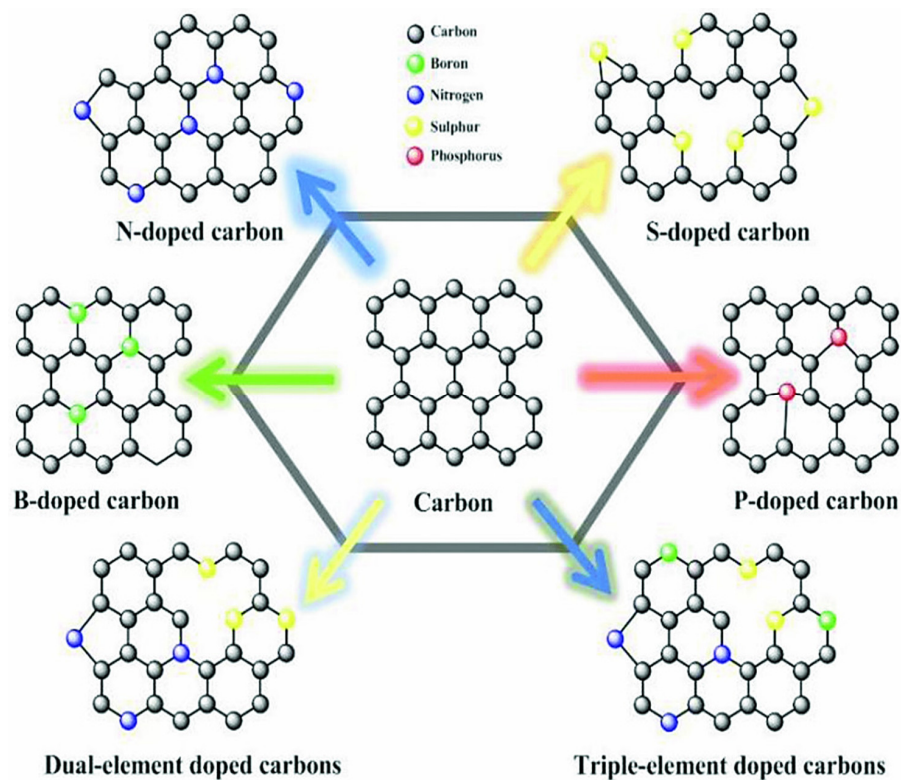


Figure 10. A schematic representation of carbon with different heteroatoms [68], open access.

Firstly, improved wettability of carbon surfaces can be achieved through surface functionalisation, as the heteroatoms on the surface create a partial positive charge, reducing the electronegativity towards the neighbouring atoms and reducing the surface polarisation. This reduced polarisation between neighbouring carbon atoms result in enhanced interactions with electrolyte ions, which ultimately improves the surface adsorption of electrolyte ions. This also reduces active materials' equivalent series resistance (ESR) when used in capacitive devices [69].

Secondly, the capacitive performance of these functionalised carbon materials can be enhanced by the pseudo-capacitive contribution made by these functional groups through fast and fully reversible Faradic redox reactions. Finally, co-doping of more than one heteroatom has been explored and found to be useful towards achieving higher capacities of supercapacitor devices, where it is anticipated that this performance improvement can be due to the synergistic contributions from these functional groups to enhance a supercapacitor cell's overall efficiency [70–72].

3.4. Composites

A very common technique to enhance the capacitive performance of SCs is to modify carbon by adding pseudo-capacitive substances, such as transition metal oxides or conducting polymers. Composites benefit from additional Faradic capacitive contribution associated with the electronic transfer originating from pseudo-capacitive materials, whereas high porosity carbons enable the improved mobility of electrolyte ions coupled with an increased number of electrochemically active sites when these pseudo-capacitive materials are deposited on the surface of the high porosity carbons and used in symmetric SCs [73,74]. Another added benefit is the higher operating voltages achieved by making hybrid supercapacitor (asymmetric SCs) devices using carbon-based anodes and battery-type cathodes, which can assist in bridging the energy gap between batteries and supercapacitors through increased operational voltages and improved capacitive performance [75]. Ternary composites, where two or more metal oxides are deposited on carbon material in order to benefit from the synergic effect between these metal oxides and carbon, have seen an increased interest recently. In a recent research study by Allado, Kokougan, et al., they synthesised a ternary composite by wrapping $\text{MnO}_2/\text{Co}_3\text{O}_4$ metal oxides around carbon fibre. Physical characterisation revealed a porous morphology of these composites, which provided channels for the movement of electrolyte ions. The assembled capacitive device displayed an excellent specific capacity of 728 Fg^{-1} using 6M KOH electrolyte, coupled with a capacity retention of 71.8% over 11,000 cycles. A high energy density of 64.5 Wh kg^{-1} at a power density of 1276 W kg^{-1} was attained [76]. Figure 11 displays various electrochemical and physical characteristics of the $\text{MnO}_2/\text{Co}_3\text{O}_4/\text{SA-ECNFs}$ composite electrode. Figure 11a shows the cyclic voltammograms (CV), which are symmetric at scan rate, indicating a good rate capability of the material; Figure 11b shows the electrochemical impedance spectroscopy (EIS) profile showing low resistance for the ternary composite; Figure 11c,d show the SEM images before and after cycling, showing the robustness of the material since there is no structural degradation; Figure 11e shows the galvanostatic charge-discharge (GCD) profile with the longer discharge time for composite; Figure 11f shows the cyclic performance.

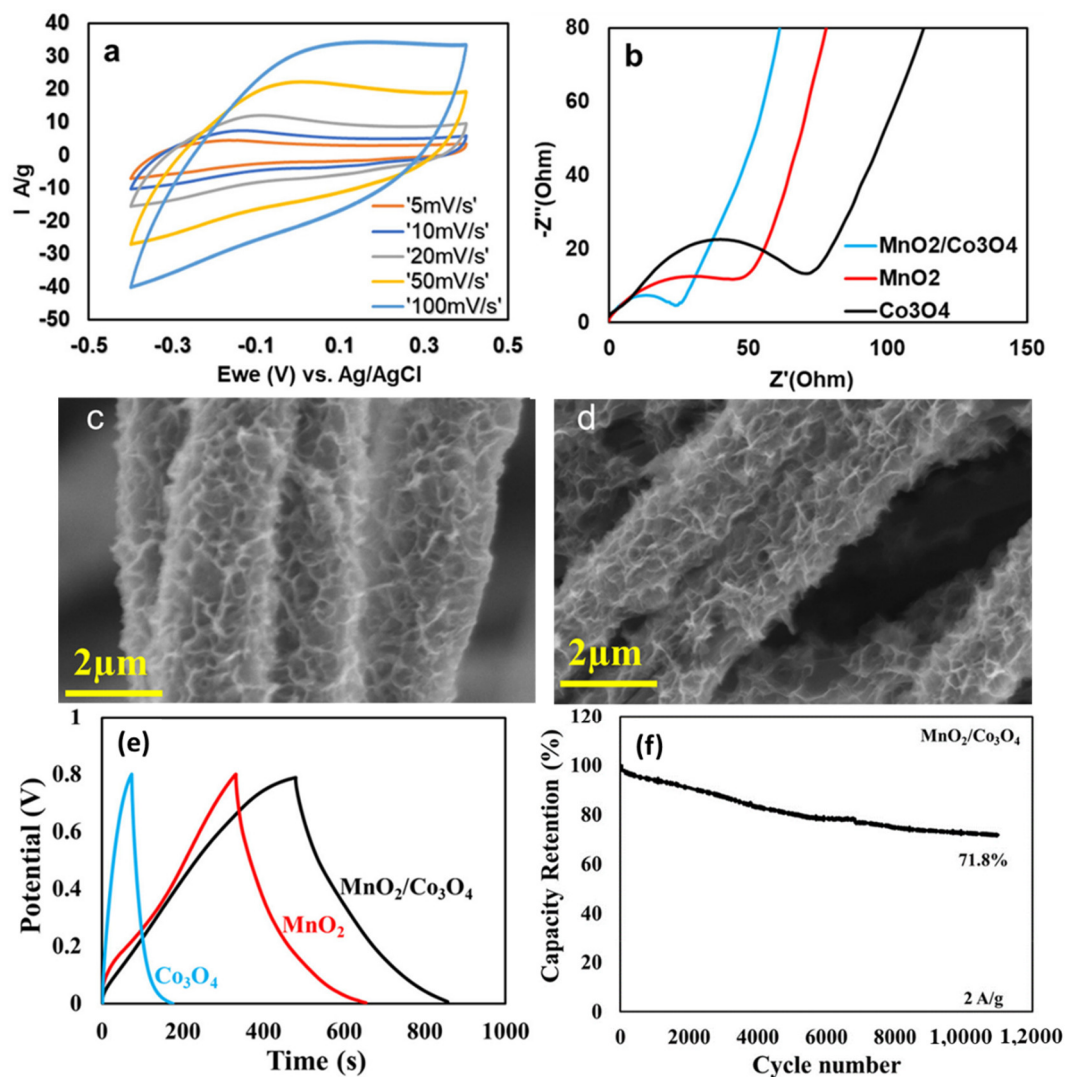


Figure 11. (a) The CV curves of $\text{MnO}_2/\text{Co}_3\text{O}_4@\text{SA-ECNFs}$; (b) the EIS spectra of different samples; (c) and (d) the SEM micrographs before and after cycling; (e) the GCD profile of different samples; and (f) the cyclic stability of $\text{MnO}_2/\text{Co}_3\text{O}_4@\text{SA-ECNFs}$ [76], open access.

4. Carbon Based Electrode Materials

Pseudo-capacitive and battery-type materials have recently seen an increased interest for their adoption as electrodes in supercapacitors due to their high energy storage capabilities. However, most of the commercially used supercapacitor devices still use carbon-based materials, particularly activated carbon, as electrodes since pseudo-capacitive and battery-type materials suffer from inferior power densities and rate-capabilities. Various carbon-based materials, whether pristine, functionalised, or as composites when used as electrodes in SCs, will be discussed in detail in the following subsections.

4.1. Graphene

Graphene, two-dimensional (2D), is a carbon nanomaterial with extraordinary physiochemical characteristics, such as high SSA, excellent electrical conductivity, mechanical strength, and very rich surface chemistry. Due to these exceptional properties, graphene has seen increased use as an active material in SC applications. Graphene was isolated from graphite using the micromechanical exfoliation technique (Scotch tape method) for the first time in 2004 by Geim and Novoselov [77]. Following the successful separation of the graphene layers from graphite, a number of other synthesis techniques have been developed and utilised by scientists in the past two decades to produce graphene. These

synthesis techniques are classified as top-down or bottom-up, depending on the synthesis route adopted. In the *top-down* method, such as exfoliation (chemical mechanical or liquid), graphene layers are separated from bulk material such as graphite by mechanical means, whereas in *bottom-up* techniques, such as chemical vapor deposition and epitaxial growth, graphene is produced through the decomposition of carbon containing precursors [78–80].

Graphene, graphene oxide, reduced graphene oxide, and its composites have been widely used as electrodes in SCs, both in academic research as well as in commercial applications. High specific surface area, excellent mechanical/chemical stabilities, chemical inertness, and rich surface chemistry are some of the highly desirable characteristics that make graphene and its derivatives and hybrids suitable active materials for electrochemical energy storage and conversion applications in general and for supercapacitors in particular [81,82]. Seo, Dong Han, et al., used vertically aligned graphene nanosheets (VGNS) as a binder-free electrode in symmetric supercapacitor cells. VGNS sheets were fabricated by the single-step, facile, and cost-effective plasma-enabled method. This uniform three-dimensional structure resulted in a high specific capacitance of 230 Fg^{-1} at 10 mVs^{-1} with a capacity retention of over 99% after 1500 cycles when used in conjunction with $0.1 \text{ M Na}_2\text{SO}_4$ aqueous electrolyte under ambient conditions [83]. Similarly, functionalised graphene has also been explored as an electrode active material in supercapacitors since heteroatom doping can enhance the overall performance of a SC cell due to the pseudo-capacitive contribution made by various functional groups alongside electric double capacitance originating from the physical interactions of electrode/electrolyte ions on the high surface area interface. In a research study, nitrogen-doped graphene was produced using a green and economical synthesis technique, where a mix of waste polyethyleneterephthalate (PET) and urea were treated hydrothermally using a novel one-step synthesis approach. An exceptionally high gravimetric capacitance of 405 Fg^{-1} at the current density of 1 Ag^{-1} was achieved when this nitrogen-doped, high-porosity graphene was used as an electrode in a supercapacitor cell. A very high energy density of 68.1 Whkg^{-1} and a high maximum power density of 558.5 Wkg^{-1} was also attained when used with a 6 M KOH electrolyte [84].

Graphene composites are widely produced using transition metal-based materials since this can provide both superior power density and energy density due to the complementary nature of these two materials. Graphene is commonly used as a host material to be doped with transition metal-based pseudo/battery-type materials; however, graphene has also been used as a dopant to improve conductivity and porous structure. Transition metal carbides and/or nitrides, also known as MXenes, have seen huge interest recently, however, sheet stacking of this two-dimensional material can result in a reduced specific surface area. Different strategies have been deployed to counter this issue, and graphene as a dopant has also been used successfully. In a study, graphene/MXenes ($\text{rGO}/\text{Ti}_3\text{C}_2\text{T}_x$) composites were fabricated by alternating filtration combined with low temperature (250°C) reduction. This composite showed excellent capacitive performance, coupled with good mechanical flexibility and outstanding cycle life. A specific capacitance of 322 Fg^{-1} was attained at 1 Ag^{-1} in $3 \text{ M H}_2\text{SO}_4$ electrolyte. These composite-based active materials have retained nearly 100% of the initial capacitance after 32,000 charge-discharge cycles, proving to be highly stable materials. Sometimes, more than two components are used to prepare composites, i.e., ternary composites, which can further enhance electrochemical performance due to the synergetic effect of each component. In another study, polyaniline/graphene/ Fe_2O_3 (PGF) nanostructured composites were synthesised; and used as an electrode material in an SC cell. This composite displayed exceptionally high capacitive performance with the specific capacitance of 1124 Fg^{-1} at a current density of 0.25 Ag^{-1} in $1 \text{ M H}_2\text{SO}_4$ electrolyte solution and displayed a good rate capability with capacitance retention of 82.2% at a much higher current density of 7.5 Ag^{-1} [85]. Various physical and electrochemical characteristics of PGF are shown in Figure 12. Figure 12a displays the complete synthesis procedure; Figure 12b displays the flakes of graphene oxide whereas; whereas Figure 12c shows Fe_2O_3 nanoparticles implanted in between graphene layers shows the composites

where polyaniline is grown alongside Fe_2O_3 nanoparticles to complete the production process of PGF. Figure 12e–g shows the outstanding electrochemical characteristics of this composite electrode active material. Figure 12e shows the charge-discharge profile and Figure 12f displays the CV curves and finally Figure 12g shows the long-term cyclability with excellent capacity retention

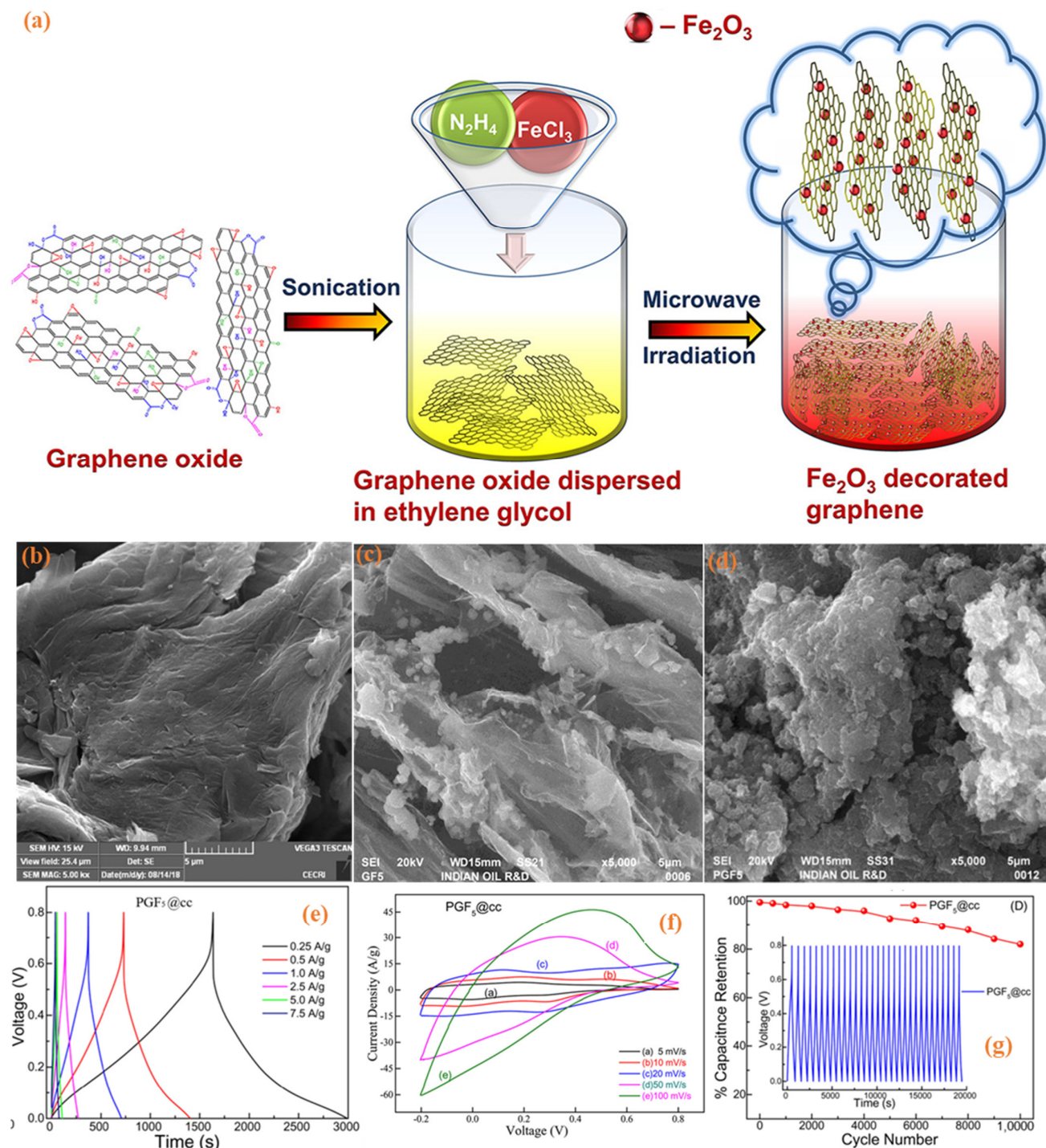


Figure 12. (a) The graphical interpretation of the synthesis of Fe_2O_3 -decorated graphene composite; the SEM micrograph of (b) graphene oxide, (c) binary composite GF, and (d) ternary composite PGF. (e) The galvanostatic charge-discharge of ternary composite PGF, (f) the cyclic voltammograms of ternary composite, and (g) the cyclic stability of ternary composite PGF over 10,000 charge-discharge cycles [85], open access.

Graphene has seen an accelerated use as an active material in SCs, as a result, graphene is currently going through a transitional phase by entering commercialization. However, it still lags behind the widely used activated carbon-based electrode materials due to the cost-effectiveness and scalability of activated carbon. Therefore, wider use of graphene in electrochemical energy storage and conversion devices in general and supercapacitor cells in particular is expected to be achieved soon. Nonetheless, new synthesis strategies and modifications in currently used production processes is required to make these procedures more economical, environmentally friendly, and scalable. Table 1 below exhibits the electrochemical performance of graphene-based electrodes.

Table 1. The electrochemical performance characteristics of graphene-based carbon electrodes.

Sample	Capacitance (Fg ⁻¹)	Energy Density (Wh kg ⁻¹)	Power Density (kW kg ⁻¹)	Retention/Cycles (%)	Ref:
VGNS	230	—	—	99/1500	[83]
rGO	585.44	81.31	62.64	97.14/5000	[86]
4NG	405	68.1	558.5	87.7/5000	[84]
NB-GO	885	23.23	872	80/10,000	[87]
NiSe	1280	50.1	816	98/2500	[88]
NiCo2S4/GA	704.34	20.9	800.2	80.3/1500	[89]
SGP	928.56	25.6	4098	77.68/11,000	[90]
MP-rGO	1942	39.1	700	78.6/3000	[91]
ZnS/RGO	772	349.7	18,000	76.1	[92]
Cu-BPA/Go	611.6	54.37	200	86/2000	[93]

4.2. Activated Carbon

AC is the most commonly used electrode active material employed in supercapacitors since it has excellent conductivity, inertness, a very high surface area, a tuneable pore size, and can be produced in large quantities cost-effectively. Carbon is produced through a high-temperature thermal treatment of synthetic materials such as polymers or naturally occurring materials, i.e., coconut shells or rice husk-based precursors under an inert environment. Another useful and efficient method of producing carbon materials is to utilise waste materials such as biomass waste and fruit residues as precursors, using a number of activation agents. These materials are not only available in abundance but also help in reducing waste and help to improve the overall environment. Carbon produced using these materials can be used in a variety of applications, including electrochemical energy storage, particularly in supercapacitors [94,95]. The porous structure of synthesised carbon can be improved even further through activation using the different activation agents discussed above in detail. The desirable characteristics required to enhance the electrochemical performance of supercapacitors include an optimised pore size according to the used electrolyte solution and a high specific surface area. The capacitive performance can be further improved with the incorporation of functional groups or by preparing the composites using pseudo-capacitive materials such as transition metal oxides or conducting polymers as dopants. This results in higher specific capacities since the total capacitance is the sum of the electric double layer capacitance originating from the surface charge storage of highly porous activated carbon and pseudo-capacitive contribution made by dopants or functional groups through fast and highly reversible Faradic charge storage. The pseudo-capacitive contribution is linked with the electronic transfer, whereas the electric double capacitance is entirely surface based and does not require a charge transfer, instead it is based on the surface adsorption-desorption of charges during cycling. MnOx/AC composites were synthesised using biomass radish as the low-cost precursor resulting in the three-dimensional crosslinked structure. These composite electrodes displayed exceptionally high capacitive performance with the gravimetric capacitance reaching 557 Fg⁻¹ at the current density of 1 Ag⁻¹ when used in conjunction with 2M KOH as an electrolyte. These composites also showed superior energy density of 248 Wh kg⁻¹ at a power density of 4786 W kg⁻¹ in

the potential range of -1 to 1 V at a current density of 1 Ag^{-1} . These hybrid electrodes also showed moderate cycle-ability with a capacity retention of approximately 47% after 10,000 charge-discharge cycles [96]. Another way of improving the performance of SCs is through the introduction of redox-active species into electrolyte solutions when they are used alongside activated carbon electrodes. An improved specific capacitance was achieved with the introduction of redox active ingredients to the electrolyte, which contributed a pseudo-capacitive element alongside the EDL capacitance contributed by the activated carbon. The specific capacitance of 885 Fg^{-1} was achieved after the addition of 0.05 M FeBr_3 to the electrolyte solution which was nearly four folds higher than 204 Fg^{-1} for the activated carbon. There was no capacity loss after 10,000 charge-discharge cycles, and it delivered a high energy density of 40 Whkg^{-1} in $0.5 \text{ M Na}_2\text{SO}_4$ [97]. Other commonly used synthesis techniques to produce highly porous activated carbon include the template-derived carbon methods. This method is commonly used by scientists in electrochemical applications in general and in supercapacitors in particular since carbons with a tuned porous structure, i.e., average pore size, specific surface area and pore volume can be produced. The template-derived carbons are of immense interest among scientists since the above-mentioned porous characteristics can have profound effect on the performance of supercapacitors [98–100]. Table 2 below displays the electrochemical characteristics of different AC based electrodes.

Table 2. The electrochemical performance characteristics of carbon electrodes.

Sample	SSA (m^2g^{-1})	APS (nm)	Capacitance (Fg^{-1})	Energy Density (Wh kg^{-1})	Power Density (kW kg^{-1})	Ref:
KOH-CX-4:1	2334	—	222	10	400	[101]
hCNC-5.0	2737	—	266	153	1000	[102]
RFCA100-800-800	1775	2.19	197	—	—	[103]
RPC	2797	1.9	56	44	564	[104]
CSAC7	1343	—	338	—	—	[105]
HAC-WS	652	2.65	225	72.2	1547.6	[106]
TiC-CDC	—	—	163	—	—	[107]

4.3. Carbon Nanotubes (CNTs)

Fundamentally, carbon can be found in different shapes and forms, such as activated carbon, graphite, and lonsdaleite. However, some novel and exotic carbon nanostructures such as graphene, carbon onions, nano-diamond, carbon nano-horns, fullerene (C_{60} , C_{240} , C_{540} and C_{20}), and carbon nanotubes (CNTs) have also been discovered and investigated in the past few decades [108]. Among all the allotropes of carbon, CNT is the most investigated due to its simplest chemical composition, atomic bonding, and diverse structural properties [109]. CNTs were first synthesised by Sumio Iijima in 1991 at the NEC Corporation using the arc discharge method, which has revolutionised many scientific fields such as physics, chemistry, and material science [110]. CNT's structure resembles that of graphene, the where basic structure is in the form of a honeycomb, similar to many other carbon allotropes. Essentially, CNTs' structure can be considered as graphene sheets rolled up into a tubular shape. CNTs can exist in two basic shapes: single "SWCNTs" (harmony with helical, armchair, and zigzag) and multi "MWCNTs" walled CNTs, depending on their nanostructure and number of concentric cylindrical layers [111]. Figure 13 illustrates the schematic of all the three types of CNTs.

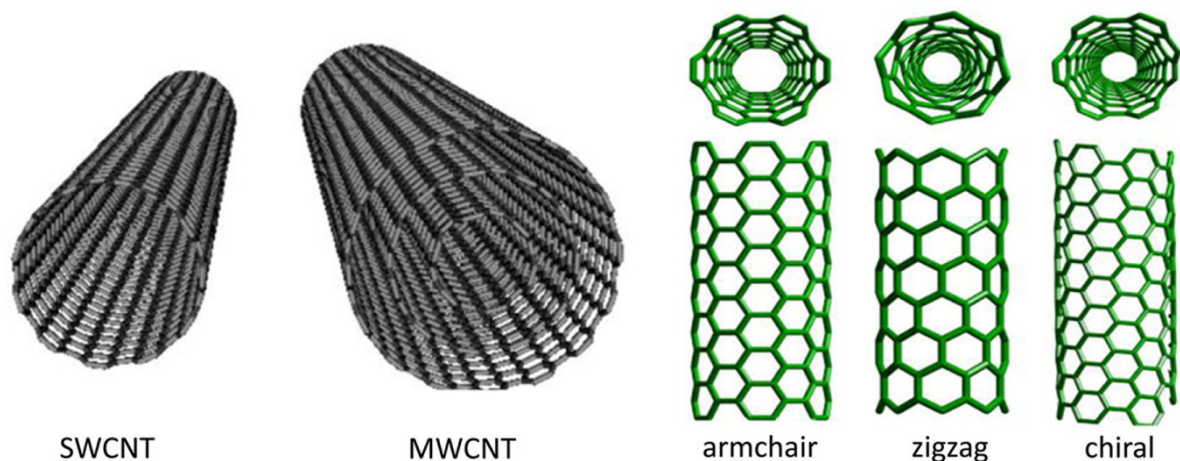


Figure 13. The graphical representation of CNTs [111], open access.

A wide range of production strategies are also being used to synthesise high-quality CNTs with diverse morphologies and structural properties. However, laser ablation, chemical vapour deposition, and arc discharge are the most commonly used techniques.

4.3.1. Arc Discharge Method

The arc discharge method is the pioneering and most widely used approach to synthesise high-quality, defect-free CNTs [112]. In this technique, the electrical breakdown of gases is used to create plasma; this process is carried out at an elevated temperature $> 1700\text{ }^{\circ}\text{C}$ resulting in high-quality, defect-free CNTs when compared with other techniques. Inert gas pressure, flow rate, and metal concentrations are the key factors that can affect the yield of CNTs. By using this method, SWCNTs of the diameter range of 0.6–1.4 nm and MWCNTs with the diameter approximately 10 nm can be produced [113,114]. Figure 14 below displays the standard setup for the arc discharge technique.

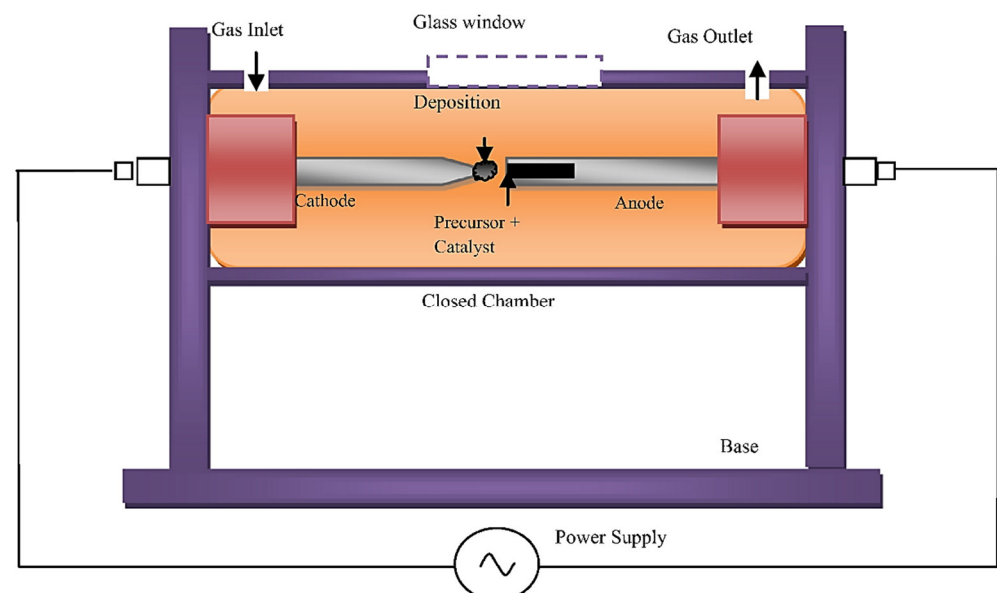


Figure 14. A graphical presentation of the arc discharge method “Reproduced with permission from [113], Elsevier, 2014”.

Even though this synthesis process is highly efficient producing excellent-quality CNTs, it has its own shortcomings, which include the utilisation of expensive noble gases, very high operating temperatures, and extremely low pressure.

4.3.2. Laser Ablation

Laser ablation is a highly useful technique for producing extremely pure, high-yield SWCNTs; however, this method is hardly used for the production of MWCNTs due to the high production cost when compared with other synthesis procedures [115]. In a typical experiment, 500 mg of a high purity SWCNTs (90% purity) can be produced in just five minutes [116]. This process uses a constant flow of a gas or mixture of inert gases such as Ar and N₂ at a temperature range of 800–1400 °C; however, 1200 °C is the most commonly used temperature, whereas the operating pressure is maintained between 200 and 400 Torr [117,118]. Figure 15 shows a laser ablation setup using ND: YAG system. When the target rod was made of pure graphite and a graphite catalyst mixture, respectively, MWCNTs and SWCNTs were formed.

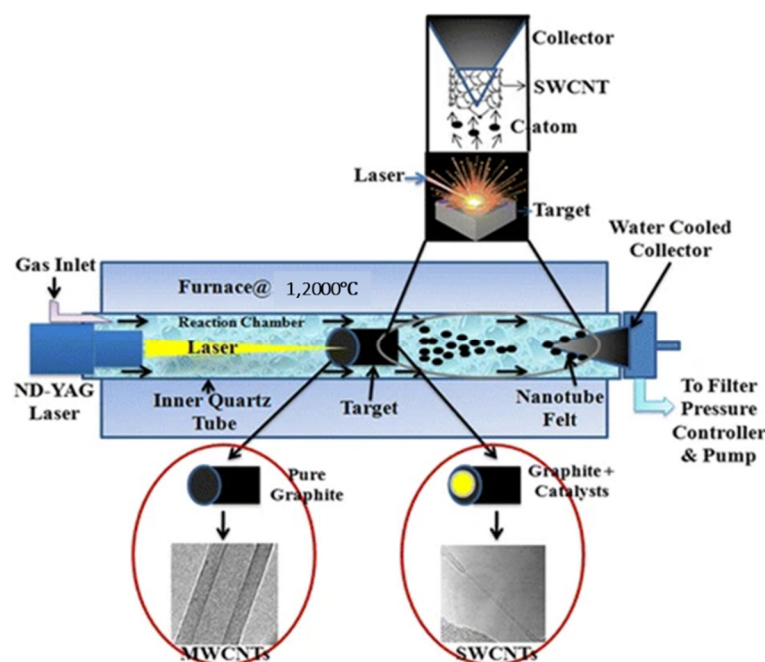


Figure 15. The schematics of a laser ablation setup to produce SWCNTs and MWCNTs [119], open access.

The properties of CNT samples produced can be affected by a variety of parameters, such as laser characteristics, target material composition, gas composition, chamber's pressure, and temperature. The main drawback of this technique is its usefulness for the production of only MWCNTs. It cannot be utilised for the production of MWCNTs due to the issues associated with production costs.

4.3.3. Chemical Vapor Deposition (CVD)

CVD is an approach that is often employed to produce allotropic carbon in general and CNTs in particular thanks to its simplicity, cost-effectiveness, ambient pressure, and lower temperatures < 1200 °C. CVD was first used in 1993, using carbon monoxide–hydrogen mixtures over Fe at 700 °C [120,121]. There are different CVD techniques such as plasma enhanced chemical vapor deposition (PACVD), microwave plasma (MPCVD), radio frequency (RF-CVD), and floating catalyst (FCCVD). Metal catalysts are a major factor that can affect the characteristics of produced CNTs samples where Pt, Fe, and Mn are used as catalysts in the form of nanoparticles with sizes less than 3 nm. Other factors, including, deposition time, temperature, and flow rate, can influence the properties of produced samples [108]. CVD is a *bottom-up* technique, unlike laser ablation and arc discharge, which are *top-down* techniques, therefore, it provides better control over the shapes and sizes of produced CNT samples.

CNTs have been studied as electrode active materials for a variety of electrochemical applications, most notably supercapacitors. As discussed earlier, CNTs can be excellent active materials for SC applications, and their performance can be enhanced even further by doping these materials with functional groups. Surface functional groups can have dual benefits, i.e., boosting the surface affinity of active materials towards electrolyte solutions (particularly aqueous electrolytes), which improves electronic conductivity, and contributing towards the overall capacitive performance of SCs by adding pseudo-capacitive components originating from nitrogen, oxygen, and sulphur functional groups. A recent study used a simple low-temperature pyrolysis technique employing HA-CoFe-ZIF to synthesize nitrogen-doped CNTs and graphene composites. This showed a high capacity of 324 F g^{-1} at a current density of 1 A g^{-1} with a high-capacity retention of 91% after 5000 cycles. Furthermore, it displayed a high energy density of 10.3 Wh kg^{-1} at 331 W kg^{-1} [122]. Various physical and electrochemical characteristics are displayed in Figure 16 below.

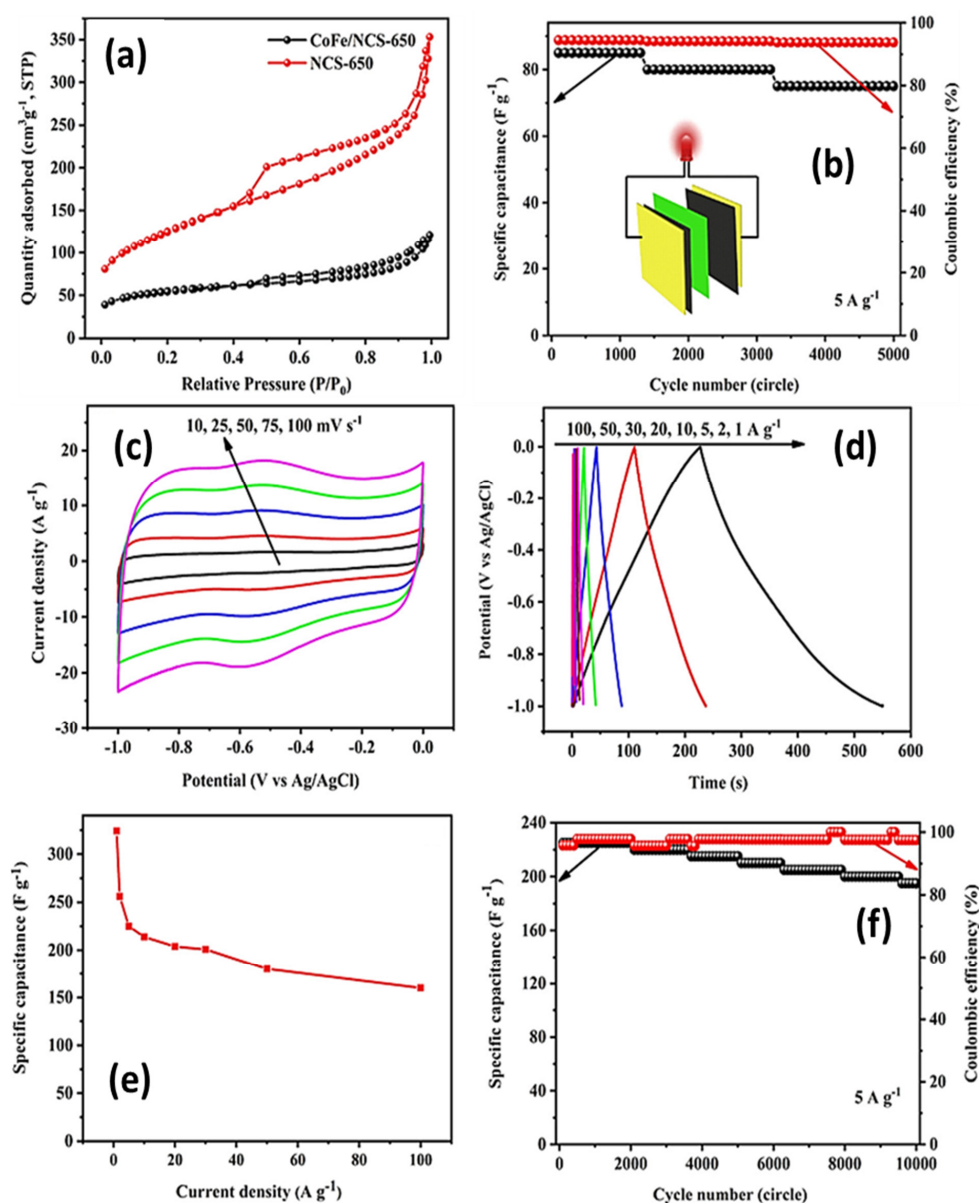


Figure 16. (a) This shows the adsorption-desorption isotherms, (b) cyclic stability and columbic efficiency of NCS-650//AC asymmetric device, (c) CV profiles at different scan rates, (d) GCD curves at different current densities, (e) specific capacitance at different current densities, and (f) cyclic stability of NCS-650 sample in three electrode setup [122], open access.

One of the fundamental issues with the wider use of SCs as an alternative power source is their high level of self-discharge compared with other electrochemical energy storage and conversion devices. Two types of self-discharges, i.e., potential driving self-discharge and diffusion control self-discharge, are the main types observed in more commercialised EDL capacitors. Nanocarbons are considered the most suited materials to study self-discharge since the charge storage in EDLCs is predominantly a surface-based physical phenomenon, unlike pseudo-capacitive materials such as transition metal oxides or conducting polymers. In a recent study by Zhang et al., they managed to control the self-discharge by tuning the surface chemistry of SWCNTs when used as active electrode material in SCs. It was found that a 13% reduction in the presence of surface function groups resulted in nearly a five-fold drop in discharge-time [123].

Similar to other carbon nanomaterials, CNTs have also been used in composite form to produce high energy/high power density electrode active materials. While CNTs assist low resistance and, therefore high-power delivery, pseudo-capacitive-battery-type electrodes provide high capacitive performance and energy density. In a recent study, Bathula and co-workers manufactured highly efficient solid-state supercapacitors based on electrode materials prepared by Co_3O_4 anchored on nitrogen-doped multiwall carbon nanotubes (NMWCNT) using a green and environmentally friendly synthesis technique. This fabricated Co_3O_4 -NMWCNT composite was investigated as an electrode in a symmetric supercapacitor cell in a 2 M KOH aqueous electrolyte. This device showed outstanding electrochemical performance, with the specific capacitance reaching 202 Fg^{-1} at the current density of 1 Ag^{-1} . This was also coupled with a high energy density of 25 Whkg^{-1} at a power density of 900 Wkg^{-1} . These results confirmed that Co_3O_4 -NMWCNT composites could be an excellent choice for high-power-high energy density supercapacitor devices [124]. Table 3 below shows the performance properties, including capacitive performance, energy and power densities, and efficiencies of CNTs and their composites when used as electrode active materials in SCs.

Table 3. The electrochemical performance characteristics of carbon nanotube electrodes.

Sample	SSA (m^2g^{-1})	Capacitance (Fg^{-1})	Energy Density (Whkg^{-1})	Power Density (Wkg^{-1})	Efficiency (%)	Ref:
NA-CNT	988	98	59	1750	91	[125]
CNT	—	489.6	56.9	9992.19	98.5	[126]
FWCNTs	142	167.7	—	—	98	[127]
P3HT/SWCNTs	—	245.8	50.8	308.7	80.5	[128]
TBN-CMP/SWCNT	1150	430	—	—	99.18	[129]
SWCNTs/ TiO_2	—	144	20	10,000	95	[130]
PC-CNTs	659.5	248	8.42	250	97.3	[131]
CNTs	205.2	—	50.1	459.9	80.1	[132]
TiO_2 -CNT	—	345.7	82.5	859	93.3	[133]
NCS	427	324	10.3	331	88	[122]

5. Conclusions and Future Prospective

Supercapacitors have emerged as suitable complementary devices in many applications, whereas in some applications, these can be used independently due to their outstanding electrochemical characteristics, including long cycle life, high power density, and good stability. An immense research drive is necessary to enhance their energy densities even further for their wider commercial applications by bringing them in line with or closer to their performance-comparable counterparts, rechargeable batteries. Various strategies have been used to improve their energy storage capabilities, including the use of a combination of different materials such as conducting polymers, transition metal oxides, and carbons as electrodes. Additionally, improvements have been achieved through the structural optimisation of carbonaceous-electrode active materials. In the current state of technology of supercapacitors, these devices can be used in applications requiring short

charging/discharging times, high cyclic stability, high power delivery, and long cycle life. It is anticipated that supercapacitor technology has a long way to go before it can achieve battery-level energy densities to replace it since energy densities of supercapacitors are much lower when compared with currently used rechargeable batteries. The future direction of research requires focusing on these key points to improve their performance even further: (a) The development of a high-porosity and highly conductive materials such as graphene, activated carbon, and carbon nanotubes in an environmentally friendly and cost-effective way since high production costs occur during the synthesis of these materials, as synthesis of these nanomaterials require very complicated and energy-intensive processes, restricting their wider industrialisation (b) The production of binary and ternary composites with the optimised composition where carbon can assist in high power delivery and can also provide large numbers of active surface area sites for the deposition of high capacity materials. These high capacity materials can be based on pseudo-capacitive or battery-type materials, which can improve the energy storage capabilities of supercapacitors to bring these devices in line with or closer to rechargeable batteries. (c) Focus should also be directed towards the electrode-electrolyte interface rather than the supercapacitor cell itself to understand the interfacial electrochemistry which can assist in enhancing their performance. (d) The development of new methodologies is also necessary to reduce self-discharge of supercapacitors, which is one of the fundamental shortcomings of these devices. (e) Hybrid devices along with metal ion supercapacitors are considered as technologies of the future requiring research attention to make these devices a commercial success by improving their power densities while maintaining their superior energy densities. (f) Currently, blade coating is a frequently used technique to deposit slurry of active materials, however, this process is very ineffective to produce light weight and thin electrode which are necessary for superior capacitive performance since most supercapacitors undergo a surface-charge storage reaction unlike rechargeable batteries where charge is stored in bulk of the material where extra un-used active material can result in inferior performance. (g) Introduction of universal testing standards in both industries and laboratories for the evaluation of supercapacitors is required so that the performance of supercapacitor cells is consistent when these devices are evaluated under different conditions. In summary, in this brief review article, we have attempted to discuss different types of supercapacitors according to their working principles and advantages and disadvantages of these devices. This was followed by the synthesis techniques of the different high-porosity carbon-based nanomaterials. Finally, the applications of carbon nanomaterials in supercapacitor devices have been discussed and recommendations for the future research direction have also been presented.

Author Contributions: Conceptualization, A.G.O., M.A.A., A.H.A. and E.T.S.; methodology Q.A., M.A.A., A.H.A., M.M. and E.T.S.; formal analysis, A.G.O., Q.A., A.H.A. and M.M.; investigation, A.G.O., M.A.A., A.H.A.; resources, A.G.O., M.A.A., A.H.A.; data curation, Q.A. and E.T.S.; writing—original draft preparation, A.G.O., Q.A., M.A.A., A.H.A., M.M. and E.T.S.; writing—review and editing, A.G.O., Q.A., M.A.A., A.H.A., M.M. and E.T.S.; supervision, A.G.O. and E.T.S.; project administration, M.A.A. and A.H.A.; All authors have read and agreed to the published version of the manuscript.

Funding: This work was supported by the University of Sharjah, Project No. 19020406129.

Institutional Review Board Statement: Not applicable.

Informed Consent Statement: Not applicable.

Data Availability Statement: Not applicable.

Conflicts of Interest: The authors declare no conflict of interest.

References

1. Naseer, A.; Hussain, M.; Shakir, I.; Abbas, Q.; Yilmaz, D.; Zahra, M.; Raza, R. The robust catalysts ($\text{Ni}_{1-x}\text{—Mo}_x$ /doped ceria and $\text{Zn}_{1-x}\text{—Mo}_x$ /doped ceria, $x = 0.1$ and 0.3) for efficient natural gas reforming in solid oxide fuel cells. *Electrochim. Acta* **2020**, *361*, 137033. [[CrossRef](#)]

2. Shabbir, I.; Mirzaeian, M.; Sher, F. Energy efficiency improvement potentials through energy benchmarking in pulp and paper industry. *Clean. Chem. Eng.* **2022**, *3*, 100058. [\[CrossRef\]](#)
3. Husin, H.; Zaki, M. A critical review of the integration of renewable energy sources with various technologies. *Prot. Control Mod. Power Syst.* **2021**, *6*, 3.
4. Wei, Z.; Zhao, J.; He, H.; Ding, G.; Cui, H.; Liu, L. Future smart battery and management: Advanced sensing from external to embedded multi-dimensional measurement. *J. Power Sources* **2021**, *489*, 229462. [\[CrossRef\]](#)
5. Wei, Z.; Hu, J.; He, H.; Yu, Y.; Marco, J. Embedded distributed temperature sensing enabled multi-state joint observation of smart lithium-ion battery. *IEEE Trans. Ind. Electron.* **2022**, *70*, 555–565. [\[CrossRef\]](#)
6. Liu, K.; Wei, Z.; Zhang, C.; Shang, Y.; Teodorescu, R.; Han, Q.-L. Towards long lifetime battery: AI-based manufacturing and management. *IEEE/CAA J. Autom. Sin.* **2022**, *9*, 1139–1165. [\[CrossRef\]](#)
7. Zhao, W.H.; Li, F.Y.; Zhang, H.X.; Eglitis, R.I.; Wang, J.; Jia, R. Doping at sp³-site in Me-graphene (C568) for new anodes in rechargeable Li-ion battery. *Appl. Surf. Sci.* **2023**, *607*, 154895. [\[CrossRef\]](#)
8. Zhang, Q.; Yan, B.; Feng, L.; Zheng, J.; You, B.; Chen, J.; Zhao, X.; Zhang, C.; Jiang, S.; He, S. Progress in the use of organic potassium salts for the synthesis of porous carbon nanomaterials: Microstructure engineering for advanced supercapacitors. *Nanoscale* **2022**, *14*, 8216–8244. [\[CrossRef\]](#)
9. Yan, B.; Feng, L.; Zheng, J.; Zhang, Q.; Jiang, S.; Zhang, C.; Ding, Y.; Han, J.; Chen, W.; He, S. High performance supercapacitors based on wood-derived thick carbon electrodes synthesized via green activation process. *Inorg. Chem. Front.* **2022**, *9*, 6108–6123. [\[CrossRef\]](#)
10. Zheng, S.; Zhang, J.; Deng, H.; Du, Y.; Shi, X. Chitin derived nitrogen-doped porous carbons with ultrahigh specific surface area and tailored hierarchical porosity for high performance supercapacitors. *J. Bioresour. Bioprod.* **2021**, *6*, 142–151. [\[CrossRef\]](#)
11. Chaparro-Garnica, J.; Salinas-Torres, D.; Mostazo-López, M.J.; Morallon, E.; Cazorla-Amorós, D. Biomass waste conversion into low-cost carbon-based materials for supercapacitors: A sustainable approach for the energy scenario. *J. Electroanal. Chem.* **2021**, *880*, 114899. [\[CrossRef\]](#)
12. Zhao, C.; Zhao, C.; Liu, Q.; Liu, X.; Lu, X.; Pang, C.; Liu, Y.; Liu, Z.; Ying, A. Investigation of the mechanism of small size effect in carbon-based supercapacitors. *Nanoscale* **2021**, *13*, 12697–12710. [\[CrossRef\]](#)
13. Wang, R.; Li, X.; Nie, Z.; Zhao, Y.; Wang, H. Metal/metal oxide nanoparticles-composited porous carbon for high-performance supercapacitors. *J. Energy Storage* **2021**, *38*, 102479. [\[CrossRef\]](#)
14. Ruiz-Montoya, J.G.; Quispe-Garrido, L.V.; Gómez, J.C.; Baena-Moncada, A.M.; Gonçalves, J.M. Recent progress in and prospects for supercapacitor materials based on metal oxide or hydroxide/biomass-derived carbon composites. *Sustain. Energy Fuels* **2021**, *5*, 5332–5365. [\[CrossRef\]](#)
15. Zhang, G.C.; Feng, M.; Li, Q.; Wang, Z.; Fang, Z.; Niu, Z.; Qu, N.; Fan, X.; Li, S.; Gu, J. High energy density in combination with high cycling stability in hybrid supercapacitors. *ACS Appl. Mater. Interfaces* **2022**, *14*, 2674–2682. [\[CrossRef\]](#)
16. Forouzandeh, P.; Kumaravel, V.; Pillai, S.C. Electrode materials for supercapacitors: A review of recent advances. *Catalysts* **2020**, *10*, 969. [\[CrossRef\]](#)
17. Liang, R.; Du, Y.; Xiao, P.; Cheng, J.; Yuan, S.; Chen, Y.; Yuan, J.; Chen, J. Transition metal oxide electrode materials for supercapacitors: A review of recent developments. *Nanomaterials* **2021**, *11*, 1248. [\[CrossRef\]](#)
18. Kumar, S.; Saeed, G.; Zhu, L.; Hui, K.N.; Kim, N.H.; Lee, J.H. 0 D to 3 D carbon-based networks combined with pseudocapacitive electrode material for high energy density supercapacitor: A review. *Chem. Eng. J.* **2021**, *403*, 126352. [\[CrossRef\]](#)
19. Qu, G.; Wang, Z.; Zhang, X.; Zhao, S.; Wang, C.; Zhao, G.; Hou, P.; Xu, X. Designing flexible asymmetric supercapacitor with high energy density by electrode engineering and charge matching mechanism. *Chem. Eng. J.* **2022**, *429*, 132406. [\[CrossRef\]](#)
20. Manasa, P.; Sambasivam, S.; Ran, F. Recent progress on biomass waste derived activated carbon electrode materials for supercapacitors applications—A review. *J. Energy Storage* **2022**, *54*, 105290. [\[CrossRef\]](#)
21. Suriyakumar, S.; Bhardwaj, P.; Grace, A.N.; Stephan, A.M. Role of polymers in enhancing the performance of electrochemical supercapacitors: A review. *Batter. Supercaps* **2021**, *4*, 571–584. [\[CrossRef\]](#)
22. Kumar, R.; Joanni, E.; Sahoo, S.; Shim, J.-J.; Kian, T.W.; Matsuda, A.; Singh, R.K. An overview of recent progress in nanostructured carbon-based supercapacitor electrodes: From zero to bi-dimensional materials. *Carbon* **2022**, *193*, 298–338. [\[CrossRef\]](#)
23. Abbas, Q.; Mirzaeian, M.; Abdelkareem, M.A.; Al Makky, A.; Yadav, A.; Olabi, A.G. Structural tuneability and electrochemical energy storage applications of resorcinol-formaldehyde-based carbon aerogels. *Int. J. Energy Res.* **2022**, *46*, 5478–5502. [\[CrossRef\]](#)
24. Abdelkareem, M.A.; Abbas, Q.; Mouselly, M.; Alawadhi, H.; Olabi, A. High-performance Effective Metal-organic Frameworks for Electrochemical Applications. *J. Sci. Adv. Mater. Devices* **2022**, *7*, 100465. [\[CrossRef\]](#)
25. Saini, S.; Chand, P.; Joshi, A. Biomass derived carbon for supercapacitor applications. *J. Energy Storage* **2021**, *39*, 102646. [\[CrossRef\]](#)
26. Jiang, G.; Senthil, R.A.; Sun, Y.; Kumar, T.R.; Pan, J. Recent progress on porous carbon and its derivatives from plants as advanced electrode materials for supercapacitors. *J. Power Sources* **2022**, *520*, 230886. [\[CrossRef\]](#)
27. Shao, Y.; El-Kady, M.F.; Sun, J.; Li, Y.; Zhang, Q.; Zhu, M.; Wang, H.; Dunn, B.; Kaner, R.B. Design and Mechanisms of Asymmetric Supercapacitors. *Chem. Rev.* **2018**, *118*, 9233–9280. [\[CrossRef\]](#)
28. Miller, E.E.; Hua, Y.; Tezel, F.H. Materials for energy storage: Review of electrode materials and methods of increasing capacitance for supercapacitors. *J. Energy Storage* **2018**, *20*, 30–40. [\[CrossRef\]](#)
29. Wei, L.; Deng, W.; Li, S.; Wu, Z.; Cai, J.; Luo, J. Sandwich-like chitosan porous carbon Spheres/MXene composite with high specific capacitance and rate performance for supercapacitors. *J. Bioresour. Bioprod.* **2022**, *7*, 63–72. [\[CrossRef\]](#)

30. Zhao, X.; He, D.; You, B. Laser engraving and punching of graphene films as flexible all-solid-state planar micro-supercapacitor electrodes. *Mater. Today Sustain.* **2022**, *17*, 100096. [\[CrossRef\]](#)
31. Zhang, L.L.; Zhao, X. Carbon-based materials as supercapacitor electrodes. *Chem. Soc. Rev.* **2009**, *38*, 2520–2531. [\[CrossRef\]](#)
32. Groß, A.; Sakong, S. Modelling the electric double layer at electrode/electrolyte interfaces. *Curr. Opin. Electrochem.* **2019**, *14*, 1–6. [\[CrossRef\]](#)
33. Wu, J. Understanding the Electric Double-Layer Structure, Capacitance, and Charging Dynamics. *Chem. Rev.* **2022**, *122*, 10821–10859. [\[CrossRef\]](#)
34. Zhai, Z.; Zhang, L.; Du, T.; Ren, B.; Xu, Y.; Wang, S.; Miao, J.; Liu, Z. A review of carbon materials for supercapacitors. *Mater. Des.* **2022**, *221*, 111017. [\[CrossRef\]](#)
35. Lv, S.; Ma, L.; Shen, X.; Tong, H. Recent design and control of carbon materials for supercapacitors. *J. Mater. Sci.* **2021**, *56*, 1919–1942. [\[CrossRef\]](#)
36. Zhao, X.; Sánchez, B.M.; Dobson, P.J.; Grant, P.S. The role of nanomaterials in redox-based supercapacitors for next generation energy storage devices. *Nanoscale* **2011**, *3*, 839–855. [\[CrossRef\]](#)
37. Augustyn, V.; Simon, P.; Dunn, B. Pseudocapacitive oxide materials for high-rate electrochemical energy storage. *Energy Environ. Sci.* **2014**, *7*, 1597–1614. [\[CrossRef\]](#)
38. Brousse, T.; Bélanger, D.; Long, J.W. To be or not to be pseudocapacitive? *J. Electrochem. Soc.* **2015**, *162*, A5185–A5189. [\[CrossRef\]](#)
39. Permatasari, F.A.; Irham, M.A.; Bisri, S.Z.; Iskandar, F. Carbon-based quantum dots for supercapacitors: Recent advances and future challenges. *Nanomaterials* **2021**, *11*, 91. [\[CrossRef\]](#)
40. Winter, M.; Brodd, R.J. What Are Batteries, Fuel Cells, and Supercapacitors? *Chem. Rev.* **2005**, *105*, 1021, Erratum in *Chem. Rev.* **2003**, *104*, 4245–4269. [\[CrossRef\]](#)
41. Herrero, E.; Buller, L.J.; Abruña, H.D. Underpotential deposition at single crystal surfaces of Au, Pt, Ag and other materials. *Chem. Rev.* **2001**, *101*, 1897–1930. [\[CrossRef\]](#) [\[PubMed\]](#)
42. Bi, R.-R.; Wu, X.-L.; Cao, F.-F.; Jiang, L.-Y.; Guo, Y.-G.; Wan, L.-J. Highly dispersed RuO₂ nanoparticles on carbon nanotubes: Facile synthesis and enhanced supercapacitance performance. *J. Phys. Chem. C* **2010**, *114*, 2448–2451. [\[CrossRef\]](#)
43. Augustyn, V.; Come, J.; Lowe, M.A.; Kim, J.W.; Taberna, P.-L.; Tolbert, S.H.; Abruña, H.D.; Simon, P.; Dunn, B. High-rate electrochemical energy storage through Li⁺ intercalation pseudocapacitance. *Nat. Mater.* **2013**, *12*, 518. [\[CrossRef\]](#) [\[PubMed\]](#)
44. Sarno, M. Nanotechnology in energy storage: The supercapacitors. In *Studies in Surface Science and Catalysis*; Elsevier: Amsterdam, The Netherlands, 2020; Volume 179, pp. 431–458.
45. Akinwolemiwa, B.; Peng, C.; Chen, G.Z. Redox electrolytes in supercapacitors. *J. Electrochem. Soc.* **2015**, *162*, A5054–A5059. [\[CrossRef\]](#)
46. Su, F.; Hou, X.; Qin, J.; Wu, Z.-S. Recent Advances and Challenges of Two-Dimensional Materials for High-Energy and High-Power Lithium-Ion Capacitors. *Batter. Supercaps* **2020**, *3*, 10–29. [\[CrossRef\]](#)
47. Nagamuthu, S.; Zhang, Y.; Xu, Y.; Sun, J.; Zhang, Y.; Zaman, F.U.; Denis, D.K.; Hou, L.; Yuan, C. Non-lithium-based metal ion capacitors: Recent advances and perspectives. *J. Mater. Chem. A* **2022**, *10*, 357–378. [\[CrossRef\]](#)
48. Song, Z.; Zhang, G.; Deng, X.; Zou, K.; Xiao, X.; Momen, R.; Massoudi, A.; Deng, W.; Hu, J.; Hou, H.; et al. Ultra-Low-Dose Pre-Metallation Strategy Served for Commercial Metal-Ion Capacitors. *Nano-Micro Lett.* **2022**, *14*, 53. [\[CrossRef\]](#)
49. Jin, L.; Shen, C.; Shellikeri, A.; Wu, Q.; Zheng, J.; Andrei, P.; Zhang, J.-G.; Zheng, J.P. Progress and perspectives on pre-lithiation technologies for lithium ion capacitors. *Energy Environ. Sci.* **2020**, *13*, 2341–2362. [\[CrossRef\]](#)
50. Wang, H.; Zhu, C.; Chao, D.; Yan, Q.; Fan, H.J. Nonaqueous Hybrid Lithium-Ion and Sodium-Ion Capacitors. *Adv. Mater.* **2017**, *29*, 1702093. [\[CrossRef\]](#)
51. Ding, J.; Hu, W.; Paek, E.; Mitlin, D. Review of Hybrid Ion Capacitors: From Aqueous to Lithium to Sodium. *Chem. Rev.* **2018**, *118*, 6457–6498. [\[CrossRef\]](#)
52. Chen, H.C.; Qin, Y.; Cao, H.; Song, X.; Huang, C.; Feng, H.; Zhao, X.S. Synthesis of amorphous nickel–cobalt–manganese hydroxides for supercapacitor-battery hybrid energy storage system. *Energy Storage Mater.* **2019**, *17*, 194–203. [\[CrossRef\]](#)
53. Sun, F.; Liu, X.; Wu, H.B.; Wang, L.; Gao, J.; Li, H.; Lu, Y. In Situ High-Level Nitrogen Doping into Carbon Nanospheres and Boosting of Capacitive Charge Storage in Both Anode and Cathode for a High-Energy 4.5 V Full-Carbon Lithium-Ion Capacitor. *Nano Lett.* **2018**, *18*, 3368–3376. [\[CrossRef\]](#) [\[PubMed\]](#)
54. Zhang, D.; Li, L.; Zhang, Y. Metal chalcogenides-based materials for high-performance metal ion capacitors. *J. Alloys Compd.* **2021**, *869*, 159352. [\[CrossRef\]](#)
55. Shakil, R.; Shaikh, M.N.; Shah, S.S.; Reaz, A.H.; Roy, C.K.; Chowdhury, A.N.; Aziz, M.A. Development of a Novel Bio-based Redox Electrolyte using Pivalic Acid and Ascorbic Acid for the Activated Carbon-based Supercapacitor Fabrication. *Asian J. Org. Chem.* **2021**, *10*, 2220–2230. [\[CrossRef\]](#)
56. Kumar, R.; Sahoo, S.; Joanni, E.; Singh, R.K. A review on the current research on microwave processing techniques applied to graphene-based supercapacitor electrodes: An emerging approach beyond conventional heating. *J. Energy Chem.* **2022**, *74*, 252–282. [\[CrossRef\]](#)
57. Jiang, K.; Gerhardt, R.A. Fabrication and Supercapacitor Applications of Multiwall Carbon Nanotube Thin Films. *C* **2021**, *7*, 70. [\[CrossRef\]](#)
58. Tiwari, A.P.; Mukhiya, T.; Muthurasu, A.; Chhetri, K.; Lee, M.; Dahal, B.; Lohani, P.C.; Kim, H.-Y. A review of electrospun carbon nanofiber-based negative electrode materials for supercapacitors. *Electrochem* **2021**, *2*, 236–250. [\[CrossRef\]](#)

59. Heidarinejad, Z.; Dehghani, M.H.; Heidari, M.; Javedan, G.; Ali, I.; Sillanpää, M. Methods for preparation and activation of activated carbon: A review. *Environ. Chem. Lett.* **2020**, *18*, 393–415. [\[CrossRef\]](#)
60. Farma, R.; Putri, A.; Taer, E.; Awitdrus, A.; Apriwandi, A. Synthesis of highly porous activated carbon nanofibers derived from bamboo waste materials for application in supercapacitor. *J. Mater. Sci. Mater. Electron.* **2021**, *32*, 7681–7691. [\[CrossRef\]](#)
61. Adan-Mas, A.; Alcaraz, L.; Arévalo-Cid, P.; López-Gómez, F.A.; Montemor, F. Coffee-derived activated carbon from second biowaste for supercapacitor applications. *Waste Manag.* **2021**, *120*, 280–289. [\[CrossRef\]](#)
62. Diaz-Terán, J.; Nevskaya, D.; Fierro, J.; Lopez-Peinado, A.; Jerez, A. Study of chemical activation process of a lignocellulosic material with KOH by XPS and XRD. *Microporous Mesoporous Mater.* **2003**, *60*, 173–181. [\[CrossRef\]](#)
63. Gao, Y.; Yue, Q.; Gao, B.; Li, A. Insight into activated carbon from different kinds of chemical activating agents: A review. *Sci. Total Environ.* **2020**, *746*, 141094. [\[CrossRef\]](#) [\[PubMed\]](#)
64. Zhang, L.; Gu, H.; Sun, H.; Cao, F.; Chen, Y.; Chen, G.Z. Molecular level one-step activation of agar to activated carbon for high performance supercapacitors. *Carbon* **2018**, *132*, 573–579. [\[CrossRef\]](#)
65. Feng, X.; Bai, Y.; Liu, M.; Li, Y.; Yang, H.; Wang, X.; Wu, C. Untangling the respective effects of heteroatom-doped carbon materials in batteries, supercapacitors and the ORR to design high performance materials. *Energy Environ. Sci.* **2021**, *14*, 2036–2089. [\[CrossRef\]](#)
66. Wang, H.; Shao, Y.; Mei, S.; Lu, Y.; Zhang, M.; Sun, J.-K.; Matyjaszewski, K.; Antonietti, M.; Yuan, J. Polymer-derived heteroatom-doped porous carbon materials. *Chem. Rev.* **2020**, *120*, 9363–9419. [\[CrossRef\]](#)
67. Mirzaei, M.; Abbas, Q.; Gibson, D.; Mazur, M. Effect of nitrogen doping on the electrochemical performance of resorcinol-formaldehyde based carbon aerogels as electrode material for supercapacitor applications. *Energy* **2019**, *173*, 809–819. [\[CrossRef\]](#)
68. Simsek, M.; Wongkaew, N. Carbon nanomaterial hybrids via laser writing for high-performance non-enzymatic electrochemical sensors: A critical review. *Anal. Bioanal. Chem.* **2021**, *413*, 6079–6099. [\[CrossRef\]](#)
69. Dujearic-Stephane, K.; Gupta, M.; Kumar, A.; Sharma, V.; Pandit, S.; Bocchetta, P.; Kumar, Y. The effect of modifications of activated carbon materials on the capacitive performance: Surface, microstructure, and wettability. *J. Compos. Sci.* **2021**, *5*, 66. [\[CrossRef\]](#)
70. Wang, K.; Chen, Y.; Liu, Y.; Zhang, H.; Shen, Y.; Pu, Z.; Qiu, H.; Li, Y. Plasma boosted N, P, O co-doped carbon microspheres for high performance Zn ion hybrid supercapacitors. *J. Alloys Compd.* **2022**, *901*, 163588. [\[CrossRef\]](#)
71. Zhou, L.; Song, F.; Yi, J.; Xu, T.; Chen, Q. Nitrogen–Oxygen Co-Doped Carbon-Coated Porous Silica/Carbon Nanotube Composites: Implications for High-Performance Capacitors. *ACS Appl. Nano Mater.* **2022**, *5*, 2175–2186. [\[CrossRef\]](#)
72. Hao, J.; Wang, J.; Qin, S.; Liu, D.; Li, Y.; Lei, W. B/N co-doped carbon nanosphere frameworks as high-performance electrodes for supercapacitors. *J. Mater. Chem. A* **2018**, *6*, 8053–8058. [\[CrossRef\]](#)
73. Rehman, Z.U.; Bilal, M.; Hou, J.; Ahmad, J.; Ullah, S.; Wang, X.; Hussain, A. Metal oxide–carbon composites for supercapacitor applications. In *Metal Oxide–Carbon Hybrid Materials*; Elsevier: Amsterdam, The Netherlands, 2022; pp. 133–177.
74. Sohoul, E.; Adib, K.; Maddah, B.; Najafi, M. Preparation of a supercapacitor electrode based on carbon nano-onions/manganese dioxide/iron oxide nanocomposite. *J. Energy Storage* **2022**, *52*, 104987. [\[CrossRef\]](#)
75. Shinde, P.A.; Chodankar, N.R.; Abdelkareem, M.A.; Patil, S.J.; Han, Y.K.; Elsaid, K.; Olabi, A.G. All Transition Metal Selenide Composed High-Energy Solid-State Hybrid Supercapacitor. *Small* **2022**, *18*, 2200248. [\[CrossRef\]](#) [\[PubMed\]](#)
76. Allado, K.; Liu, M.; Jayapalan, A.; Arvapalli, D.; Nowlin, K.; Wei, J. Binary MnO₂/Co₃O₄ metal oxides wrapped on superaligned electrospun carbon nanofibers as binder free supercapacitor electrodes. *Energy Fuels* **2021**, *35*, 8396–8405. [\[CrossRef\]](#)
77. Novoselov, K.S.; Geim, A.K.; Morozov, S.V.; Jiang, D.-E.; Zhang, Y.; Dubonos, S.V.; Grigorieva, I.V.; Firsov, A.A. Electric field effect in atomically thin carbon films. *Science* **2004**, *306*, 666–669. [\[CrossRef\]](#)
78. Kumar, N.; Salehiyan, R.; Chauke, V.; Bothoko, O.J.; Setshedi, K.; Scriba, M.; Masukume, M.; Ray, S.S. Top-down synthesis of graphene: A comprehensive review. *FlatChem* **2021**, *27*, 100224. [\[CrossRef\]](#)
79. Olatomiwa, A.L.; Adam, T.; Gopinath, S.C.; Kolawole, S.Y.; Olayinka, O.H.; Hashim, U. Graphene synthesis, fabrication, characterization based on bottom-up and top-down approaches: An overview. *J. Semicond.* **2022**, *43*, 061101. [\[CrossRef\]](#)
80. Choi, S.H.; Yun, S.J.; Won, Y.S.; Oh, C.S.; Kim, S.M.; Kim, K.K.; Lee, Y.H. Large-scale synthesis of graphene and other 2D materials towards industrialization. *Nat. Commun.* **2022**, *13*, 1484. [\[CrossRef\]](#)
81. Bai, L.; Zhang, Y.; Tong, W.; Sun, L.; Huang, H.; An, Q.; Tian, N.; Chu, P.K. Graphene for energy storage and conversion: Synthesis and interdisciplinary applications. *Electrochem. Energy Rev.* **2020**, *3*, 395–430. [\[CrossRef\]](#)
82. Jiang, Y.; Guo, F.; Liu, Y.; Xu, Z.; Gao, C. Three-dimensional printing of graphene-based materials for energy storage and conversion. *SusMat* **2021**, *1*, 304–323. [\[CrossRef\]](#)
83. Seo, D.H.; Han, Z.J.; Kumar, S.; Ostrikov, K. Structure-controlled, vertical graphene-based, binder-free electrodes from plasma-reformed butter enhance supercapacitor performance. *Adv. Energy Mater.* **2013**, *3*, 1316–1323. [\[CrossRef\]](#)
84. Ellessawy, N.A.; El Nady, J.; Wazeer, W.; Kashyout, A. Development of high-performance supercapacitor based on a novel controllable green synthesis for 3D nitrogen doped graphene. *Sci. Rep.* **2019**, *9*, 1129. [\[CrossRef\]](#) [\[PubMed\]](#)
85. Gupta, A.; Sardana, S.; Dalal, J.; Lather, S.; Maan, A.S.; Tripathi, R.; Punia, R.; Singh, K.; Ohlan, A. Nanostructured polyaniline/graphene/Fe₂O₃ composites hydrogel as a high-performance flexible supercapacitor electrode material. *ACS Appl. Energy Mater.* **2020**, *3*, 6434–6446. [\[CrossRef\]](#)

86. Karaman, O.; Kariper, İ.A.; Korkmaz, S.; Karimi-Maleh, H.; Usta, M.; Karaman, C. Irradiated rGO electrode-based high-performance supercapacitors: Boosting effect of GO/rGO mixed nanosheets on electrochemical performance. *Fuel* **2022**, *328*, 125298. [\[CrossRef\]](#)
87. Prakash, D.; Manivannan, S. N. B co-doped and crumpled graphene oxide pseudocapacitive electrode for high energy supercapacitor. *Surf. Interfaces* **2021**, *23*, 101025. [\[CrossRef\]](#)
88. Kirubasankar, B.; Murugadoss, V.; Lin, J.; Ding, T.; Dong, M.; Liu, H.; Zhang, J.; Li, T.; Wang, N.; Guo, Z. In situ grown nickel selenide on graphene nanohybrid electrodes for high energy density asymmetric supercapacitors. *Nanoscale* **2018**, *10*, 20414–20425. [\[CrossRef\]](#)
89. Li, B.; Tian, Z.; Li, H.; Yang, Z.; Wang, Y.; Wang, X. Self-supporting graphene aerogel electrode intensified by NiCo₂S₄ nanoparticles for asymmetric supercapacitor. *Electrochim. Acta* **2019**, *314*, 32–39. [\[CrossRef\]](#)
90. Vandana, M.; Veeresh, S.; Ganesh, H.; Nagaraju, Y.; Vijeth, H.; Basappa, M.; Devendrappa, H. Graphene oxide decorated SnO₂ quantum dots/polypyrrole ternary composites towards symmetric supercapacitor application. *J. Energy Storage* **2022**, *46*, 103904. [\[CrossRef\]](#)
91. Hao, J.; Liu, H.; Han, S.; Lian, J. MoS₂ nanosheet-polypyrrole composites deposited on reduced graphene oxide for supercapacitor applications. *ACS Appl. Nano Mater.* **2021**, *4*, 1330–1339. [\[CrossRef\]](#)
92. Xu, Z.; Zhang, Z.; Yin, H.; Hou, S.; Lin, H.; Zhou, J.; Zhuo, S. Investigation on the role of different conductive polymers in supercapacitors based on a zinc sulfide/reduced graphene oxide/conductive polymer ternary composite electrode. *RSC Adv.* **2020**, *10*, 3122–3129. [\[CrossRef\]](#)
93. Goda, E.S.; Hong, S.E.; Yoon, K.R. Facile synthesis of Cu-PBA nanocubes/graphene oxide composite as binder-free electrodes for supercapacitor. *J. Alloys Compd.* **2021**, *859*, 157868. [\[CrossRef\]](#)
94. Obey, G.; Adelaide, M.; Ramaraj, R. Biochar derived from non-customized matamba fruit shell as an adsorbent for wastewater treatment. *J. Bioresour. Bioprod.* **2022**, *7*, 109–115. [\[CrossRef\]](#)
95. Jjagwe, J.; Olupot, P.W.; Menya, E.; Kalibbala, H.M. Synthesis and application of Granular activated carbon from biomass waste materials for water treatment: A review. *J. Bioresour. Bioprod.* **2021**, *6*, 292–322. [\[CrossRef\]](#)
96. Zhou, H.; Zhan, Y.; Guo, F.; Du, S.; Tian, B.; Dong, Y.; Qian, L. Synthesis of biomass-derived carbon aerogel/MnOx composite as electrode material for high-performance supercapacitors. *Electrochim. Acta* **2021**, *390*, 138817. [\[CrossRef\]](#)
97. Wang, Y.; Chang, Z.; Qian, M.; Zhang, Z.; Lin, J.; Huang, F. Enhanced specific capacitance by a new dual redox-active electrolyte in activated carbon-based supercapacitors. *Carbon* **2019**, *143*, 300–308. [\[CrossRef\]](#)
98. Yan, B.; Zheng, J.; Wang, F.; Zhao, L.; Zhang, Q.; Xu, W.; He, S. Review on porous carbon materials engineered by ZnO templates: Design, synthesis and capacitance performance. *Mater. Des.* **2021**, *201*, 109518. [\[CrossRef\]](#)
99. Vivo-Vilches, J.F.; Karakashov, B.; Celzard, A.; Fierro, V.; El Hage, R.; Brosse, N.; Dufour, A.; Etienne, M. Carbon Monoliths with Hierarchical Porous Structure for All-Vanadium Redox Flow Batteries. *Batteries* **2021**, *7*, 55. [\[CrossRef\]](#)
100. Wang, P.; Zhang, G.; Chen, W.; Chen, Q.; Jiao, H.; Liu, L.; Wang, X.; Deng, X. Molten salt template synthesis of hierarchical porous nitrogen-containing activated carbon derived from chitosan for CO₂ capture. *ACS Omega* **2020**, *5*, 23460–23467. [\[CrossRef\]](#)
101. Chavhan, M.P.; Slovak, V.; Zelenkova, G.; Dominko, D. Revisiting the Effect of Pyrolysis Temperature and Type of Activation on the Performance of Carbon Electrodes in an Electrochemical Capacitor. *Materials* **2022**, *15*, 2431. [\[CrossRef\]](#)
102. Li, G.; Chen, Y.; Yan, L.; Gong, Q.; Chen, G.; Yang, L.; Wu, Q.; Wang, X.; Hu, Z. The Composite-Template Method to Construct Hierarchical Carbon Nanocages for Supercapacitors with Ultrahigh Energy and Power Densities. *Small* **2022**, *18*, 2107082. [\[CrossRef\]](#)
103. Abbas, Q.; Mirzaei, M.; Ogburn, A.A.; Mazur, M.; Gibson, D. Effect of physical activation/surface functional groups on wettability and electrochemical performance of carbon/activated carbon aerogels based electrode materials for electrochemical capacitors. *Int. J. Hydrogen Energy* **2020**, *45*, 13586–13595. [\[CrossRef\]](#)
104. Xu, S.-W.; Zhang, M.-C.; Zhang, G.-Q.; Liu, J.-H.; Liu, X.-Z.; Zhang, X.; Zhao, D.-D.; Xu, C.-L.; Zhao, Y.-Q. Temperature-dependent performance of carbon-based supercapacitors with water-in-salt electrolyte. *J. Power Sources* **2019**, *441*, 227220. [\[CrossRef\]](#)
105. Cheng, J.; Hu, S.-C.; Sun, G.-T.; Kang, K.; Zhu, M.-Q.; Geng, Z.-C. Comparison of activated carbons prepared by one-step and two-step chemical activation process based on cotton stalk for supercapacitors application. *Energy* **2021**, *215*, 119144. [\[CrossRef\]](#)
106. Wei, H.; Wang, H.; Li, A.; Li, H.; Cui, D.; Dong, M.; Lin, J.; Fan, J.; Zhang, J.; Hou, H. Advanced porous hierarchical activated carbon derived from agricultural wastes toward high performance supercapacitors. *J. Alloys Compd.* **2020**, *820*, 153111. [\[CrossRef\]](#)
107. Käärik, M.; Arulepp, M.; Kozlova, J.; Aruväli, J.; Mäeorg, U.; Kikas, A.; Kisand, V.; Tamm, A.; Leis, J. Effect of partial oxidation and repolarization of TiC-derived nanoporous carbon electrodes on supercapacitor performance using a pH-neutral aqueous electrolyte. *J. Solid State Electrochem.* **2022**, *26*, 2365–2378. [\[CrossRef\]](#)
108. Salah, L.S.; Ouslimani, N.; Bousba, D.; Huynen, I.; Danlée, Y.; Aksas, H. Carbon nanotubes (CNTs) from synthesis to functionalized (CNTs) using conventional and new chemical approaches. *J. Nanomater.* **2021**, *2021*, 4972770. [\[CrossRef\]](#)
109. Gupta, N.; Gupta, S.M.; Sharma, S. Carbon nanotubes: Synthesis, properties and engineering applications. *Carbon Lett.* **2019**, *29*, 419–447. [\[CrossRef\]](#)
110. Kanu, N.J.; Bapat, S.; Deodhar, H.; Gupta, E.; Singh, G.K.; Vates, U.K.; Verma, G.C.; Pandey, V. An insight into processing and properties of smart carbon nanotubes reinforced nanocomposites. *Smart Sci.* **2022**, *10*, 40–55. [\[CrossRef\]](#)
111. Madani, S.Y.; Mandel, A.; Seifalian, A.M. A concise review of carbon nanotube's toxicology. *Nano Rev.* **2013**, *4*, 21521. [\[CrossRef\]](#)

112. Ribeiro, H.; Schnitzler, M.C.; da Silva, W.M.; Santos, A.P. Purification of carbon nanotubes produced by the electric arc-discharge method. *Surf. Interfaces* **2021**, *26*, 101389. [\[CrossRef\]](#)
113. Arora, N.; Sharma, N. Arc discharge synthesis of carbon nanotubes: Comprehensive review. *Diam. Relat. Mater.* **2014**, *50*, 135–150. [\[CrossRef\]](#)
114. Zhang, Y.-F. A review of arc-discharge method towards large-scale preparation of long linear carbon chains. *Chin. Phys. B* **2022**, *31*, 125201. [\[CrossRef\]](#)
115. Herrera-Ramirez, J.M.; Perez-Bustamante, R.; Aguilar-Elguezabal, A. An overview of the synthesis, characterization, and applications of carbon nanotubes. In *Carbon-Based Nanofillers and Their Rubber Nanocomposites*; Elsevier: Amsterdam, The Netherlands, 2019; pp. 47–75.
116. Santangelo, S. Controlled surface functionalization of carbon nanotubes by nitric acid vapors generated from sub-azeotropic solution. *Surf. Interface Anal.* **2016**, *48*, 17–25. [\[CrossRef\]](#)
117. Shoukat, R.; Khan, M.I. Carbon nanotubes/nanofibers (CNTs/CNFs): A review on state of the art synthesis methods. *Microsyst. Technol.* **2022**, *28*, 885–901. [\[CrossRef\]](#)
118. Kim, M.; Osone, S.; Kim, T.; Higashi, H.; Seto, T. Synthesis of nanoparticles by laser ablation: A review. *KONA Powder Part. J.* **2017**, *34*, 80–90. [\[CrossRef\]](#)
119. Das, R.; Shahnavaz, Z.; Ali, M.; Islam, M.M.; Abd Hamid, S.B. Can we optimize arc discharge and laser ablation for well-controlled carbon nanotube synthesis? *Nanoscale Res. Lett.* **2016**, *11*, 510. [\[CrossRef\]](#)
120. José-Yacamán, M.; Miki-Yoshida, M.; Rendon, L.; Santiesteban, J. Catalytic growth of carbon microtubules with fullerene structure. *Appl. Phys. Lett.* **1993**, *62*, 657–659. [\[CrossRef\]](#)
121. Tempel, H.; Joshi, R.; Schneider, J.J. Ink jet printing of ferritin as method for selective catalyst patterning and growth of multiwalled carbon nanotubes. *Mater. Chem. Phys.* **2010**, *121*, 178–183. [\[CrossRef\]](#)
122. He, F.; Li, K.; Cong, S.; Yuan, H.; Wang, X.; Wu, B.; Zhang, R.; Chu, J.; Gong, M.; Xiong, S. Design and synthesis of N-doped carbon skeleton assembled by carbon nanotubes and graphene as a high-performance electrode material for supercapacitors. *ACS Appl. Energy Mater.* **2021**, *4*, 7731–7742. [\[CrossRef\]](#)
123. Zhang, Q.; Cai, C.; Qin, J.; Wei, B. Tunable self-discharge process of carbon nanotube based supercapacitors. *Nano Energy* **2014**, *4*, 14–22. [\[CrossRef\]](#)
124. Bathula, C.; Rabani, I.; Ramesh, S.; Lee, S.-H.; Palem, R.R.; Ahmed, A.T.A.; Kim, H.S.; Seo, Y.-S.; Kim, H.-S. Highly efficient solid-state synthesis of Co₃O₄ on multiwalled carbon nanotubes for supercapacitors. *J. Alloys Compd.* **2021**, *887*, 161307. [\[CrossRef\]](#)
125. Yun, Y.S.; Yoon, G.; Kang, K.; Jin, H.-J. High-performance supercapacitors based on defect-engineered carbon nanotubes. *Carbon* **2014**, *80*, 246–254. [\[CrossRef\]](#)
126. Kariper, İ.A.; Korkmaz, S.; Karaman, C.; Karaman, O. High energy supercapacitors based on functionalized carbon nanotubes: Effect of atomic oxygen doping via various radiation sources. *Fuel* **2022**, *324*, 124497. [\[CrossRef\]](#)
127. Alvarenga, D.F.; Junior, M.G.; Santos, M.C.; Pinto, P.S.; da Cunha, T.H.; Dias, M.C.; Lavall, R.L.; Ortega, P.F. Tuning carbon nanotube-based buckypaper properties by incorporating different cellulose nanofibrils for redox supercapacitor electrodes. *J. Energy Storage* **2022**, *52*, 104848. [\[CrossRef\]](#)
128. Shokry, A.; Karim, M.; Khalil, M.; Ebrahim, S.; El Nady, J. Supercapacitor based on polymeric binary composite of polythiophene and single-walled carbon nanotubes. *Sci. Rep.* **2022**, *12*, 11278. [\[CrossRef\]](#) [\[PubMed\]](#)
129. Samy, M.M.; Mohamed, M.G.; El-Mahdy, A.F.; Mansoure, T.H.; Wu, K.C.-W.; Kuo, S.-W. High-performance supercapacitor electrodes prepared from dispersions of tetrabenzonaphthalene-based conjugated microporous polymers and carbon nanotubes. *ACS Appl. Mater. Interfaces* **2021**, *13*, 51906–51916. [\[CrossRef\]](#)
130. Lal, M.S.; Badam, R.; Matsumi, N.; Ramaprabhu, S. Hydrothermal synthesis of single-walled carbon nanotubes/TiO₂ for quasi-solid-state composite-type symmetric hybrid supercapacitors. *J. Energy Storage* **2021**, *40*, 102794. [\[CrossRef\]](#)
131. Wang, D.; Chen, Y.; Wang, H.; Zhao, P.; Liu, W.; Wang, Y. N-doped porous carbon anchoring on carbon nanotubes derived from ZIF-8/polypyrrole nanotubes for superior supercapacitor electrodes. *Appl. Surf. Sci.* **2018**, *457*, 1018–1024. [\[CrossRef\]](#)
132. Fan, L.-Q.; Tu, Q.-M.; Geng, C.-L.; Wang, Y.-L.; Sun, S.-J.; Huang, Y.-F.; Wu, J.-H. Improved redox-active ionic liquid-based ionogel electrolyte by introducing carbon nanotubes for application in all-solid-state supercapacitors. *Int. J. Hydrogen Energy* **2020**, *45*, 17131–17139. [\[CrossRef\]](#)
133. Li, J.; Ao, J.; Zhong, C.; Yin, T. Three-dimensional nanobranched TiO₂-carbon nanotube for high performance supercapacitors. *Appl. Surf. Sci.* **2021**, *563*, 150301. [\[CrossRef\]](#)

Disclaimer/Publisher's Note: The statements, opinions and data contained in all publications are solely those of the individual author(s) and contributor(s) and not of MDPI and/or the editor(s). MDPI and/or the editor(s) disclaim responsibility for any injury to people or property resulting from any ideas, methods, instructions or products referred to in the content.